



## 1   **In situ measurements of cloud microphysics and aerosol over 2   coastal Antarctica during the MAC campaign**

3

4   **Sebastian J. O'Shea<sup>1</sup>, Thomas W. Choularton<sup>1</sup>, Michael Flynn<sup>1</sup>, Keith N. Bower<sup>1</sup>,**  
5   **Martin Gallagher<sup>1</sup>, Jonathan Crosier<sup>1,2</sup>, Ian Crawford<sup>3</sup>, Zoë Fleming<sup>4</sup>, Constantino**  
6   **Listowski<sup>4\*</sup>, Amélie Kirchgaessner<sup>4</sup>, Russell S. Ladkin<sup>4</sup>, and Thomas Lachlan-Cope<sup>4</sup>**

7

8   [1]{School of Earth and Environmental Sciences, University of Manchester, Oxford Road,  
9   Manchester, M13 9PL, UK}

10   [2]{National Centre for Atmospheric Science, University of Manchester, Oxford Road,  
11   Manchester, M13 9PL, UK}

12   [3]{National Centre for Atmospheric Science, Department of Chemistry, University of  
13   Leicester, Leicester, LE1 7RH, UK}

14   [4]{British Antarctic Survey, NERC, High Cross, Madingley Rd, Cambridge CB3 0ET, UK}

15   \*now at: LATMOS/IPSL, UVSQ Université Paris-Saclay, UPMC Univ. Paris 06, CNRS,  
16   Guyancourt, France

17   Correspondence to: S. J. O'Shea (sebastian.oshea@manchester.ac.uk)

18

### 19   **Abstract**

20   During austral summer 2015 the Microphysics of Antarctic Clouds (MAC) field campaign  
21   collected detailed airborne and ground based in situ measurements of cloud and aerosol  
22   properties over coastal Antarctica and the Weddell Sea. This paper presents the first results  
23   from the experiment and discusses the key processes important in this region.

24   The sampling was predominantly of stratus cloud, at temperatures between -20 and 0 °C.  
25   These clouds were dominated by supercooled liquid water droplets, which had a median  
26   concentration of 113 cm<sup>-3</sup> and an inter-quartile range of 86 cm<sup>-3</sup>. The concentration of large  
27   aerosols (0.5 to 1.6 µm) decreased with altitude and were depleted in airmasses that originated



1 over the Antarctic Continent compared to those more heavily influenced by the Southern  
2 Ocean and sea ice regions. The dominant aerosol in the region was hygroscopic in nature,  
3 with the hygroscopicity parameter,  $\kappa$  having a median value for the campaign of 0.64  
4 (interquartile range = 0.34). This is consistent with other remote marine locations that are  
5 dominated by sea salt/sulphate.

6 Cloud ice particle concentrations were highly variable with the ice tending to occur in small  
7 isolated patches. Below ca 2000 m glaciated cloud regions were more common at higher  
8 temperatures; however the clouds were still predominantly liquid throughout. When ice was  
9 present at temperatures higher than -10 °C, secondary ice production most likely through the  
10 Hallet-Mossop mechanism lead to ice concentrations 1 to 3 orders of magnitude higher than  
11 the number predicted by commonly used primary ice nucleation parameterisations. The  
12 drivers of the ice crystal variability are investigated. No clear dependence on the droplet size  
13 distribution was found. However, higher ice concentrations were found in updrafts and  
14 downdrafts compared to quiescent regions. The source of first ice in the clouds remains  
15 uncertain, but may include contributions from biogenic particles, blowing snow or other  
16 surface ice production mechanisms.

17

## 18 **1 Introduction**

19 Antarctic clouds have a central role in the weather and climate at high southern latitudes  
20 (Lubin et al., 1998; Lawson and Gettelman, 2014). Through snow precipitation and their  
21 radiative effects they are key to the mass balance of the Antarctic ice sheet, which impacts on  
22 global sea levels (van den Broeke et al., 2011) and Southern Ocean circulation (Bromwich et  
23 al., 2012). In addition it has been suggested that changes in Antarctic clouds can influence  
24 weather patterns as far away as the tropics and even the extratropics of the Northern  
25 Hemisphere (Lubin et al., 1998).

26 Despite their importance Antarctic clouds are some of the least studied of any region around  
27 the globe (Bromwich et al., 2012). The remote location and harsh conditions cause significant  
28 logistical challenges for field projects in this region. As a consequence there is evidence that  
29 clouds and their radiative properties are poorly represented in weather and climate models  
30 over Antarctica (Bromwich et al., 2013; King et al., 2015) and the Southern Ocean (Bodas-  
31 Salcedo et al., 2012; 2016).



Key uncertainties concern the aerosol in the region, in particular the number and sources of cloud condensation nuclei (CCN) and ice nucleating particles (INPs). Conventional parameterisations predicting INP concentrations have primarily been developed using measurements at mid-latitudes (e.g. Cooper, 1986; DeMott et al., 2010) and may not be appropriate for Antarctica. A number of intensive field campaigns have been conducted studying Arctic clouds (McFarquhar and Cober, 2004; McFarquhar et al., 2007; Verlinde et al., 2007; Lloyd et al., 2015a), however analogies between the polar regions may also not be appropriate. The Arctic receives significant anthropogenic aerosol input due to its proximity to industrial nations, and is therefore likely to have significantly different type and number of CCN/INP (Mauritsen et al., 2011; Lathem et al., 2013; Liu et al., 2015).

To date, Antarctic INP measurements have mostly been made at surface sites. Measurements of snowflake residuals at the South Pole identified the long range transport of clays as the likely dominant source (Kumai, 1976). However, interpretation of these measurements is complicated due to secondary aerosol scavenging by the snowflakes and precipitation, meaning they contain particles in addition to the original nuclei. More recently, filter samples at the South Pole detected INPs that were active between -18 and -27°C, with concentrations of  $1 \text{ L}^{-1}$  at -23 °C. Mineral dusts transported from the Patagonian deserts were identified as the likely source (Ardon-Dryer et al., 2011). A synthesis of INP measurements prior to 1988 from the high southern latitudes ( $> 60^\circ\text{S}$ ), found mean concentrations between  $2 \times 10^{-4}$  and  $0.2 \text{ L}^{-1}$  at -15°C (Bigg, 1990). Given the general absence of other local INP sources, biogenic INPs may have a more important role in the Antarctic than in other regions. Biological species (pollen, bacteria, fungal spores and plankton) have been shown to act as INP at significantly higher temperatures than mineral dusts ( $> -15^\circ\text{C}$ ) (Möhler et al., 2007; Alpert et al., 2011; Murray et al., 2012; Amato et al., 2015; Wilson et al., 2015). However, Antarctic snowfall has been shown to be relatively depleted of biological INP (Christner et al., 2008) and bacteria commonly found in sea ice may not be effective INP (Junge and Swanson, 2007). The few in situ measurements of Antarctic clouds to date have suggested the importance of secondary ice processes (Grosvenor et al., 2012; Lachlan-Cope et al., 2016).

There is a clear need for more direct measurements to test and improve the representation of Antarctic clouds in climate/weather models. This paper presents both ground based and airborne measurements of cloud and aerosol properties during the 2015 Microphysics of Antarctic Clouds (MAC) field campaign aimed at addressing this. Section 2 provides an



1 overview of the campaign and the measurement techniques used. Section 3 presents a  
2 statistical overview of the aerosol and cloud observations using all available measurements.  
3 Section 4 discusses the key microphysical processes. Conclusions are presented in Sect. 5.

4

## 5 **2 Methods**

### 6 **2.1 Campaign and meteorological overview**

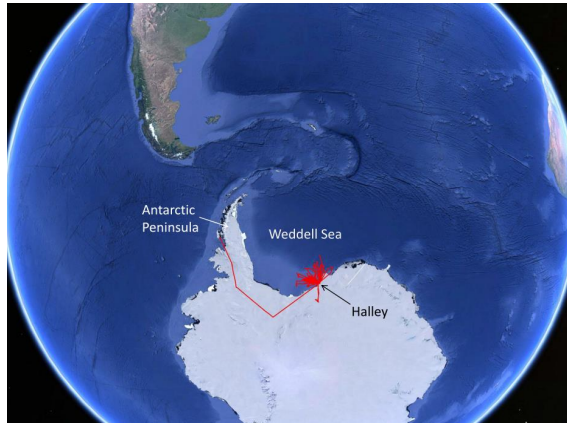
7 The MAC experiment comprised both airborne and ground based measurements of cloud and  
8 aerosol properties. Ground based measurements were performed at the Clean Air Sector  
9 Laboratory (CASLab), which is located at the Halley research station. Halley is a coastal  
10 Antarctic base on the Brunt Ice shelf, approximately 30 km from the Weddell Sea ( $75.6^{\circ}$  S,  
11  $26.7^{\circ}$  W). The CASLab is located 1 km south of the main Halley buildings and receives  
12 minimal pollution from the base and vehicle traffic due to the prevailing easterly wind (Jones  
13 et al., 2008). All CASLab measurements were filtered using the wind direction to help  
14 remove any remaining influence from the base.

15 The airborne measurements were collected using the British Antarctic Survey's Twin Otter  
16 MASIN research aircraft (King et al., 2008). Twenty-four flights (a total of 80 hours) were  
17 performed during November and December 2015 from Halley. These flights have the nominal  
18 flight numbers 212 to 235. The flights were predominantly performed over the Weddell Sea  
19 (see Fig. 1), which at this time and location was covered by a mixture of broken sea ice and  
20 polynyas. This is shown in Fig. 1 together with the sea ice fraction from the Nimbus-7  
21 Multichannel Microwave Radiometer (SMMR) and Defense Meteorological Satellite Program  
22 (DMSP) SSM/I-SSMIS passive microwave data (Cavalieri et al., 1996.) One flight sampled  
23 clouds in-land over the Antarctic continent (Flight 233). In addition a transit took place from  
24 Rothera research station on the Antarctic Peninsula (Flights 212 to 215); however not all  
25 instruments were available during these transit flights. Since the aircraft was not pressurised,  
26 the measurements were restricted to altitudes below approximately 4000 m. As a  
27 consequence, the majority of clouds were sampled over the temperature range -11 and -3 °C  
28 (79%). Seventeen percent of in-cloud measurements were collected at temperatures below -11  
29 °C and 4% at temperatures higher than -3 °C. In total 17 hours of sampling during the  
30 campaign was performed in-cloud.

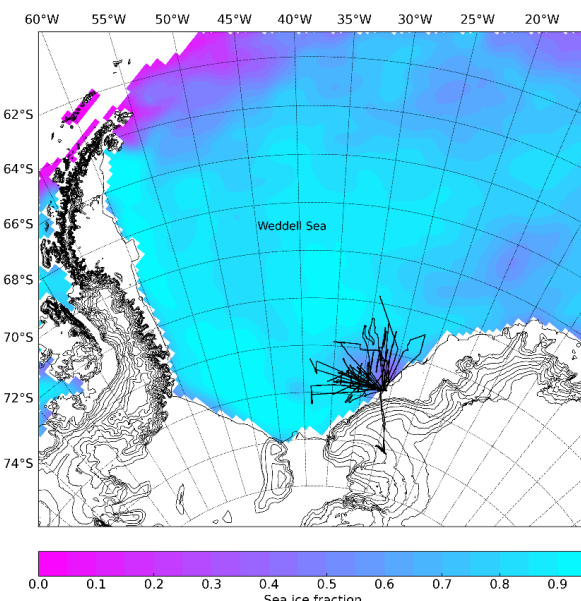
31



1



2



3

4 *Figure 1. Top panel: Flight tracks during the MAC field project (source Google Earth).*  
5 *Lower panel: shows the sea ice fraction on the Weddell Sea (Cavalieri et al., 1996) during the*  
6 *experimental period.*

7



1 The clouds sampled were generally stratiform. The exception to this was Flight 224, which  
2 sampled frontal clouds. Back trajectory analysis showed that two broad regimes were present  
3 during the project. The earlier flights (up to Flight 223) generally sampled airmasses that had  
4 travelled south over the Southern Ocean and Weddell Sea. Later in the campaign there was a  
5 transition to airmasses with greater influence from the Antarctic continent.

6 **2.2 Aircraft**

7 During MAC the Twin Otter MASIN research aircraft was fitted with a range of in situ  
8 aerosol and cloud microphysical instrumentation. Cloud particle size distributions were  
9 derived using the images from two optical array probes (OAP): a 2DS (2D-stereo, SPEC Inc.,  
10 USA, see Lawson et al., 2006) with a nominal size range of 10 to 1280 µm (10 µm pixel  
11 resolution) and a CIP-25 (Cloud Imaging Probe, DMT Inc., USA, Baumgardner et al., 2001)  
12 with a size range of 25 to 1600 µm (25 µm pixel resolution).

13 Particle size distributions over the size range from 0.5 to 50 µm were recorded using a Cloud  
14 Aerosol Spectrometer (CAS, DMT Inc., USA, Baumgardner et al., 2001). The CAS sizing  
15 was calibrated by the manufacturer using polystyrene latex (PSL) spheres (< 2 µm) and glass  
16 beads (> 2 µm) (Baumgardner et al., 2014). During MAC the sizing of the CAS's larger bins  
17 (>10 µm) was also validated using reference glass calibration beads and show little instrument  
18 drift (see Fig 2.).

19 The aircraft was also fitted with a Cloud Droplet Probe (CDP-100, DMT Inc.) for observing  
20 cloud droplets between 3 and 50 µm (Lance et al., 2010). Following the method detailed by  
21 Rosenberg et al. (2012), glass beads were used to determine the CDP's size bin centres and  
22 widths. The 2DS, CIP-25 and CAS were fitted with anti-shatter tips to minimise ice break-up  
23 on their leading edges (Korolev et al., 2011). For full details of the data processing and  
24 quality control of the 2DS and CIP-25 measurements see Crosier et al. (2011) and Taylor et  
25 al. (2016). It should be noted that in addition to the use of anti-shatter tips, an inter-arrival  
26 time algorithm was used to further reduce shattering artefacts on the 2DS and CIP-25  
27 datasets. Ice mass content was determined from the 2DS and CIP-25 images using the Brown  
28 and Francis (1995) mass-diameter relationship. As an example Fig. 2 shows a comparison  
29 between the CDP, CAS, 2DS, and CIP-25 size distributions for Flight 227. Unless stated  
30 otherwise all flight data presented has been averaged to 10 second intervals.

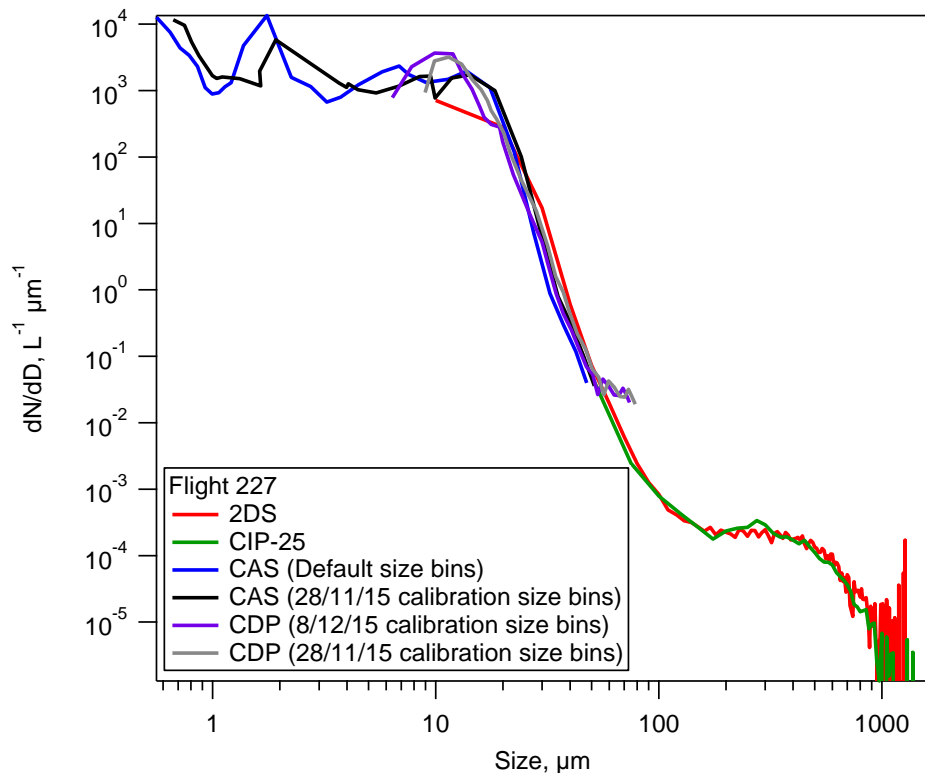


Figure 2. Average size distribution for Flight 227 comparing the 2DS, CIP-25 CDP and CAS probes. The CAS and CDP shows the Flight 227 size distributions using results from the bead calibrations performed during the campaign in order to monitor instrument performance.

Following Crosier et al. (2011), 2DS images were classified based on a geometric analysis of their circularity. Particles containing less than 50 pixels (equivalent to a diameter of approximately 80  $\mu\text{m}$ ) were not classified since they contain insufficient pixels to accurately determine their shape. Particles with circularity values less than 1.2 were classified as low irregular (LI) and are indicative of liquid drops. Circularities greater than 1.4 are associated with ice crystals and are classified as high irregular (HI). Visual inspection of the LI and HI images confirmed that they were almost all liquid droplets and ice crystals, respectively. Circularities between 1.2 and 1.4 are classified as medium irregular (MI). Interpretation of the MI category with respect to the particle phase is more ambiguous than the other categories. In general, the MI images were of quasi-spherical ice crystals, such as



recently frozen drops, however they may also include some poorly imaged liquid drops that should be classified as LI. During MAC the concentration of MI particles was generally significantly less than HI particles. The mean ratio HI:MI for the campaign was 7 (see also Sect. 3.1). This suggests that the HI concentration is likely a good proxy for the ice crystal concentration. However to highlight the uncertainty in the phase separation, in Sect. 3 the MI concentration is also shown along with the HI concentration.

Aerosol instrumentation on the aircraft included a GRIMM optical particle counter (GRIMM Model 1.109) capable of detecting aerosol particles over the size range from 0.25 to 32  $\mu\text{m}$ . The GRIMM sampled through a Brechtel Model 1200 isokinetic aerosol inlet with a >95% sampling efficiency for particles in the size range 0.01  $\mu\text{m}$  to 6  $\mu\text{m}$ . Inlet losses only become significant for particles >6  $\mu\text{m}$  and here we only consider the concentration of particles below 2  $\mu\text{m}$ . Total aerosol concentrations of particles >10 nm in size were determined using a Condensation Particle Counter (CPC, TSI Inc. Model 3772).

The aircraft was also fitted with instrumentation to measure temperature, turbulence, humidity, radiation and surface temperature. See King et al. (2008) for full details.

### 2.3 Ground site measurements

Aerosol instrumentation was installed at the CASLab sampling from its central aerosol stack (Jones et al., 2008) for the measurement period from 27 November 2015 to 15 December 2015. A Scanning Mobility Particle Sizer (SMPS, TSI) was used to generate a quasi-monodisperse aerosol flow. The SMPS performed 27 discrete steps over the aerosol size range from 30 to 500 nm. Downstream of the SMPS the flow ( $1 \text{ L}^{-1}$ ) was split isokinetically between a cloud condensation nuclei counter (CCNc, Droplet Measurement Technology Model CCN-100) and a condensation particle counter (CPC, TSI). The CCN concentration was measured at super saturations of 0.05%, 0.13%, 0.20%, 0.26% and 0.34%. The activated cloud droplet fraction was determined by the ratio of activated particles from the CCN to the total number of particles measured by the CPC. The dry diameter at which 50% of particles were activated ( $D_{50}$ ) was determined by fitting a sigmoid curve to the activated fraction size spectrum (Whitehead et al., 2016). The total CCN concentration was determined by integrating the concentration of particles larger than  $D_{50}$ . The hygroscopicity parameter  $\kappa$  was derived from  $\kappa$ -Köhler theory using the  $D_{50}$  and supersaturation values (Petters and Kreidenweis, 2007).



1 The SMPS and CCNc were calibrated at the beginning and end of the campaign (Good et al.,  
2 2010). The SMPS was size calibrated using NIST traceable polystyrene latex spheres (PSLs).  
3 Ammonium sulphate and sodium chloride were used to calibrate the CCNc supersaturations,  
4 by comparing measured values to theoretical ones from the Aerosol Diameter Dependent  
5 Equilibrium Model (ADDEM) (Topping et al., 2005).  
6 Additional measurements were provided by an Aerodynamic Particle Sizer (TSI Model 3321)  
7 which provided aerodynamic particle size concentration measurements over the size range  
8  $0.5 < D < 20 \mu\text{m}$  and in the size range  $0.3 < D < 20 \mu\text{m}$  from simultaneous aerosol scattering cross  
9 section measurements.  
10 Continuous measurements of airborne bio-fluorescent particle concentrations (primary  
11 biological and mixed biological and non-biological) were also made at CASLab using a  
12 Wideband Integrated Bioaerosol Spectrometer (WIBS Model Dstl-3, Gabey et al. 2010,  
13 Crawford et al. 2014, 2015). Measurements from this instrument will be described in detail in  
14 a separate paper.  
15

### 16 3 Results

#### 17 3.1 Cloud microphysics

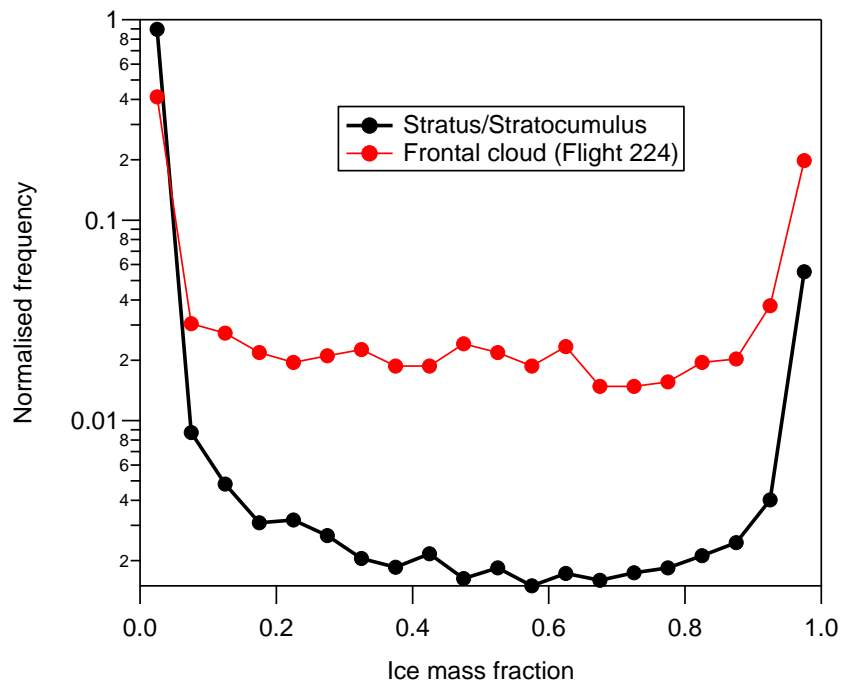
18 The following section presents a broad overview of the microphysical measurements during  
19 the MAC field campaign. For this analysis “in-cloud” measurements were determined as  
20 periods when the liquid water content (LWC) was greater than  $0.01 \text{ g m}^{-3}$  or when particles  
21 were detected by the 2DS. Flight 224 is excluded from this bulk analysis since this flight  
22 sampled frontal cloud, while the other flights sampled shallow layer cloud. The ice mass  
23 fraction (IMF) is calculated as the ratio of the ice mass to the total condensed water. Here the  
24 ice mass is taken as the sum of the HI and MI 2DS categories, while the liquid mass is taken  
25 as the sum of the CAS droplets ( $>3 \mu\text{m}$ ) and the 2DS LI category. Ice mass fractions of 0 and  
26 1 represent fully liquid and glaciated conditions, respectively. Figure 3 (black line) shows the  
27 frequency distribution of ice mass fraction based on all 1 Hz measurements in layer clouds  
28 sampled during MAC. As can be seen in Fig. 3 the clouds were dominated by liquid water.  
29 Ice mass fractions between 0 and 0.1 were observed 90% of the time, while only 6% of cases  
30 had values between 0.9 and 1. Figure 4 shows the ice mass fraction as a function of height,  
31 the black line shows the mean for each altitude bin. For altitudes below ca. 2000 m there is a



1 general trend of glaciated conditions becoming more prevalent with decreasing altitude (and  
2 increasing temperature). At temperatures higher than -3 °C glaciated conditions (IMF greater  
3 than 0.9) were responsible for 15% of observations, compared to 7% at temperatures between  
4 -8 and -3 °C. Above 2000m glaciated regions become more frequent with increasing altitude,  
5 however this is based on comparatively few observations.

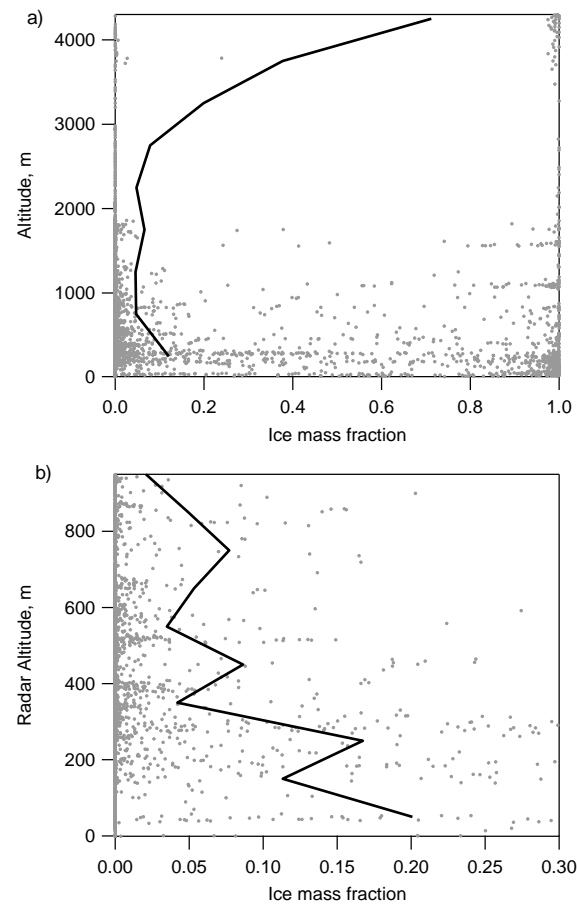
6 Measurements in Arctic stratus/stratocumulus generally find these clouds to be similarly  
7 dominated by liquid drops (McFarquhar and Cober, 2004; McFarquhar et al., 2007; Lloyd et  
8 al., 2015a). McFarquhar et al. (2007) also show a trend of increasing IMF with increasing  
9 distance from cloud top (and increasing temperature) during the Mixed-Phase Arctic Cloud  
10 Experiment (M-PACE). Glaciated conditions were observed during 23% of their  
11 measurements. This is significantly more than during MAC, possibly due to lower INP  
12 concentrations available for primary ice development in the Antarctic compared to the Arctic.

13 Flight 224 sampled cloud layers at the rear of an occluded front that was associated with a  
14 low pressure system north of Halley. Several layers were observed between -19 °C and -1 °C  
15 with ice crystals precipitating between the layers. As shown in Fig. 3 (red line) ice was more  
16 frequently observed in these clouds than during the flights where stratocumulus/stratus clouds  
17 were sampled. Twenty-four percent of measurements had ice mass fractions between 0.9 and  
18 1, while 32% of observed ice mass fraction values were between 0.1 and 0.9. Droplet number  
19 concentrations were comparatively low with a mean of 40 (29 at 1 $\sigma$ ) cm<sup>-3</sup>.



1

2 *Figure 3. Frequency distribution of the 1 Hz cloud ice mass fraction measurements.*



1           2 *Figure 4. Ice mass fraction as a function of altitude, black lines show the average ice mass*  
2           3 *fraction for each altitude bin.*

4

5       The droplet number concentration as a function of temperature is shown in Fig. 5a. This was  
6       found to be relatively consistent and temperature independent during the campaign with a  
7       median of  $113 \text{ cm}^{-3}$  and an inter-quartile range of  $86 \text{ cm}^{-3}$ . An exception to this is Flight 217,  
8       when anomalously high droplet concentrations were observed at  $-23^\circ\text{C}$  (mean  $310 \text{ cm}^{-3}$ ). The  
9       2DS was not available during this flight but the CIP observations suggest that ice was not  
10      present in this cloud. The reason for the enhanced droplet concentrations is not clear, however  
11      the aerosol concentrations below the cloud layer was similarly elevated with the CPC  
12      recording concentrations of over  $1200 \text{ scm}^{-3}$ , compared to the median for the campaign of 408

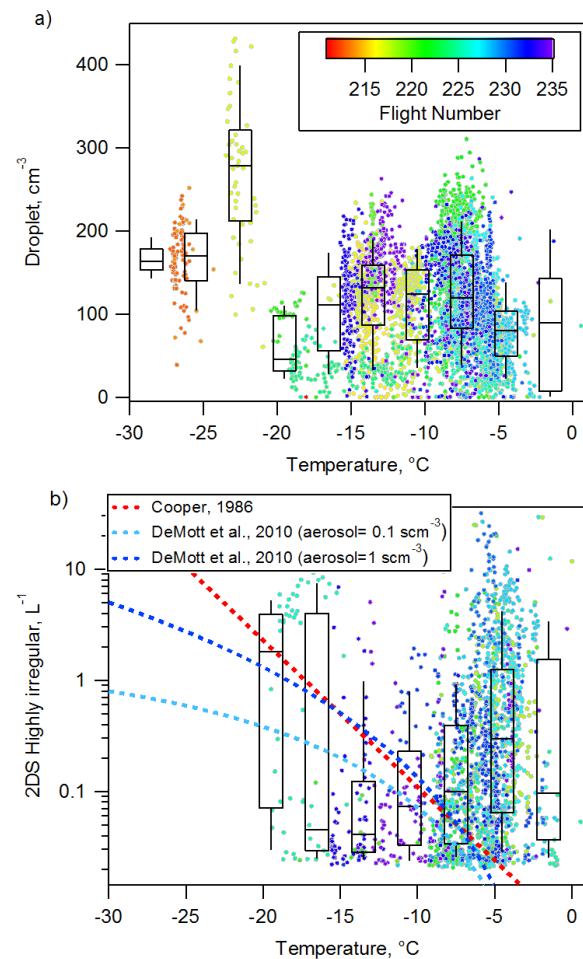


1     $\text{scm}^{-3}$ . Back trajectory analysis showed that in the previous days this airmass travelled over  
2    the Southern Ocean from South America.

3    The cloud droplet concentrations during MAC are found to be comparable with previous  
4    observations from the Antarctic Peninsula (Lachlan-Cope et al., 2016) and also Arctic  
5    summer stratocumulus (Lloyd et al., 2015a). Droplet concentrations over the Antarctic  
6    Peninsula varied between 60 and 200  $\text{cm}^{-3}$  (Lachlan-Cope et al., 2016). Concentrations on the  
7    eastern side of the Peninsula were moderately higher than on the west, which may be due to  
8    the greater sea ice coverage on the eastern side. It has been suggested that sea ice may provide  
9    a more efficient source of sea-salt aerosol, and therefore CCN, than open waters (Yang et al.,  
10   2008). Recent measurements and modelling found that sea ice made a significant contribution  
11   to the winter sea-salt aerosol loading at coastal (Dumont d'Urville) and central (Concordia)  
12   East Antarctic sites (Legrand et al., 2016).

13   The number of highly irregular particles observed by the 2DS can be used as a proxy for the  
14   number of ice crystals; it is shown as a function of temperature in Fig. 5b. Box and whisker  
15   plots show statistics for those regions of the cloud where ice is present (i.e. excluding regions  
16   with only liquid cloud water). The 2DS was not operated during the flights previous to flight  
17   218 so measurements are only available at temperatures higher than -20 °C. The two lowest  
18   temperature bins in Fig. 5b show the highest concentration of ice crystals. However these  
19   measurements come from only one flight (Flight 226) where the base (4000 m) of high cloud  
20   was sampled. These crystals (predominantly rosettes and aggregates) are highly likely to have  
21   been nucleated at lower temperatures higher up in the cloud which then sedimented down to  
22   be sampled by the aircraft. Above -15 °C there is a trend of the ice crystal concentrations  
23   showing greater variability and higher median concentrations with increasing temperature. Ice  
24   in the clouds tended to occur in small patches. A histogram of the spatial extent of ice patches  
25   shows that they increase in frequency with decreasing length up to the maximum resolvable  
26   by the 2DS measurements (a sampling frequency of 10s corresponds to a spatial scale of ca  
27   600m).

28



1

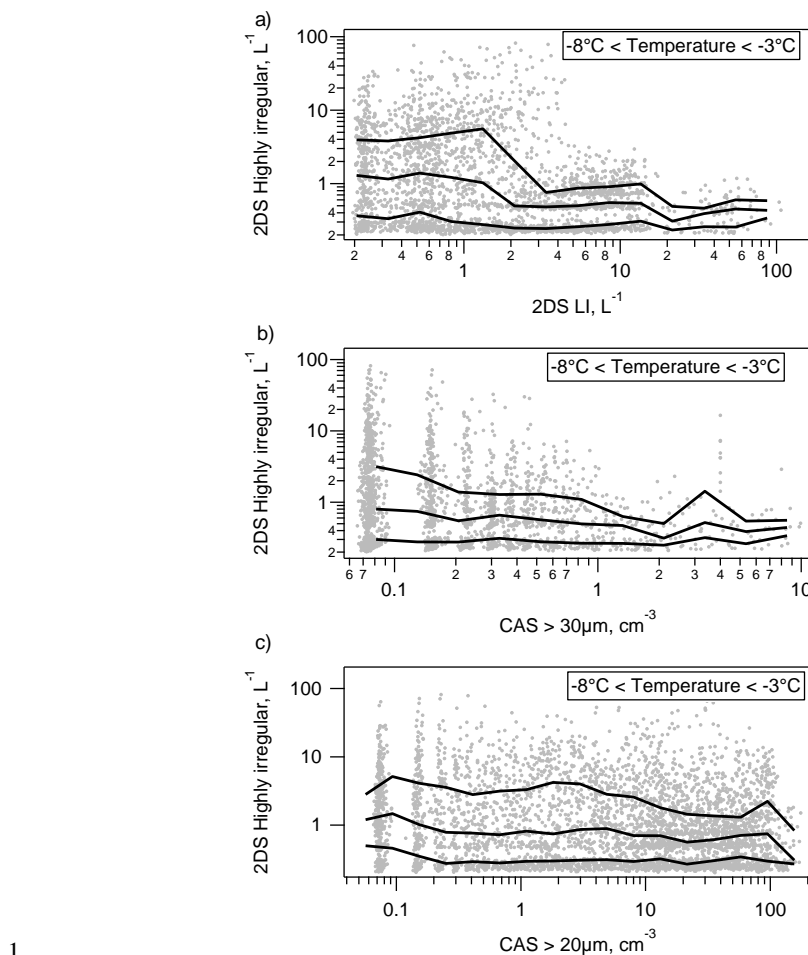
2 *Figure 5. Box and whisker plots summarising in cloud measurements (averaged over 10 s) as*  
3 *a function of temperature. Plate a) shows the concentration of cloud droplets ( $\text{cm}^{-3}$ ),*  
4 *measured by CAS, while b) shows the concentration of ice particles measured by 2DS, based*  
5 *on those classified as highly irregular (see text for details). The concentration of ice*  
6 *nucleating particles predicted by the DeMott et al. (2010) parameterisation with a high (1*  
7  *$\text{cm}^{-3}$ ) and low ( $0.1 \text{ cm}^{-3}$ ) aerosol input are shown as dark and light blue lines, respectively in*  
8 *b). The red line is the predicted ice particle concentration according to the Cooper (1986)*  
9 *parameterisation.*

10



1 Previous observations of Arctic mixed phase clouds found that the presence of precipitating  
2 ice particles ( $> 400 \mu\text{m}$ ) was associated with the number of large drops ( $>30 \mu\text{m}$ ), however  
3 the precise nucleation mechanism through which this occurs is uncertain (Lance et al., 2011).  
4 To identify if a similar relationship was present during MAC Fig. 6a shows the relationship  
5 between the 2DS HI and the 2DS LI particles (droplets larger than approximately  $80 \mu\text{m}$ ) over  
6 the temperature range -8 to -3 °C. Figures 6b and 6c show similar plots for the CAS  
7 measurements of droplets larger than 30 and 20  $\mu\text{m}$ , respectively. The HI concentrations are  
8 binned based on the droplet concentration and the 25, 50 and 75 percentiles are shown as  
9 black lines. When examining statistics for all stratus flights we find no evidence that the ice  
10 concentrations increase due to the presence of large drops. However, any relationship may be  
11 obscured as drops are depleted by ice crystal growth through riming and the Wegener-  
12 Bergeron-Findeisen process.

13



2     *Figure 6a. The relationship between the concentration of highly irregular (2DS HI) particles  
3     and low irregular particles (2DS LI) (low irregular particles greater than approximately 80  
4     μm) for the temperature range -8 to -3 °C. Figures 6b and 6c show the relationship with the  
5     concentration of droplets larger than 30 and 20 μm, respectively. The black lines are the 25th,  
6     50th and 75th percentile of the 2DS HI concentration for each droplet concentration bin.*

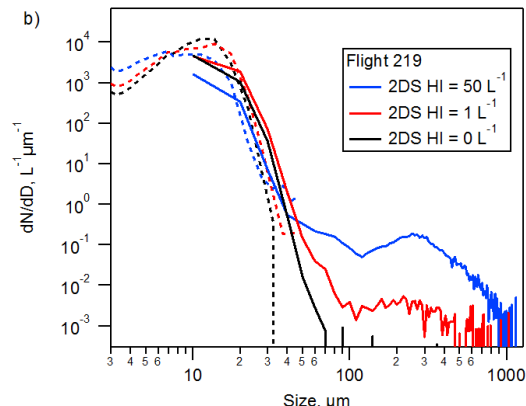
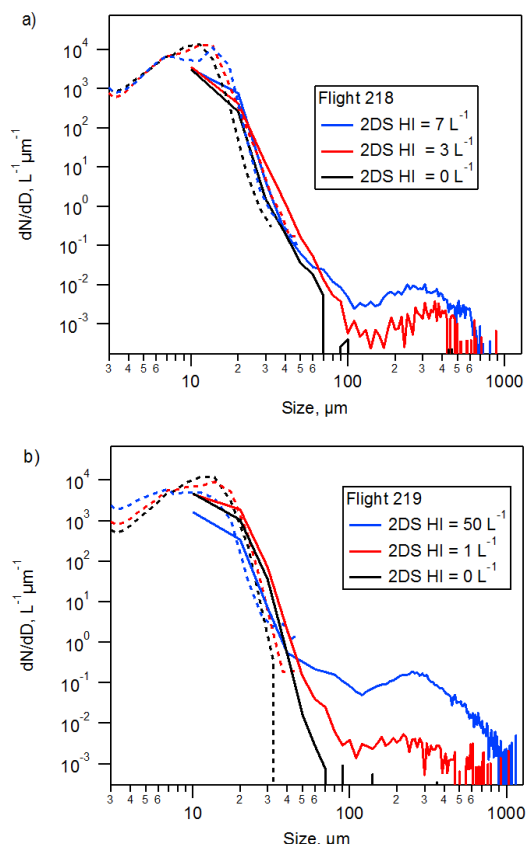
7

8     Similar results are found when case studies for individual flights are examined. Figure 7a  
9     shows a comparison between the particle size distributions for three periods with quite  
10    different degrees of glaciation during a constant altitude run at -5 °C during Flight 218. Time  
11    series of the microphysical properties during this run are shown in Fig. 8. During this run



1 there were patches of ice with concentrations of several per litre and regions where no ice was  
2 present. However, there are no distinct differences in the droplet spectrum for these three  
3 cases. Figure 7b shows a similar plot for a constant altitude run at -6 °C during Flight 219.  
4 During times with very high ice concentrations (2DS HI up to  $50 \text{ L}^{-1}$ , blue line) the droplets  
5 are depleted compared to the cases when the 2DS HI concentration was  $1 \text{ L}^{-1}$  and  $0 \text{ L}^{-1}$ .

6

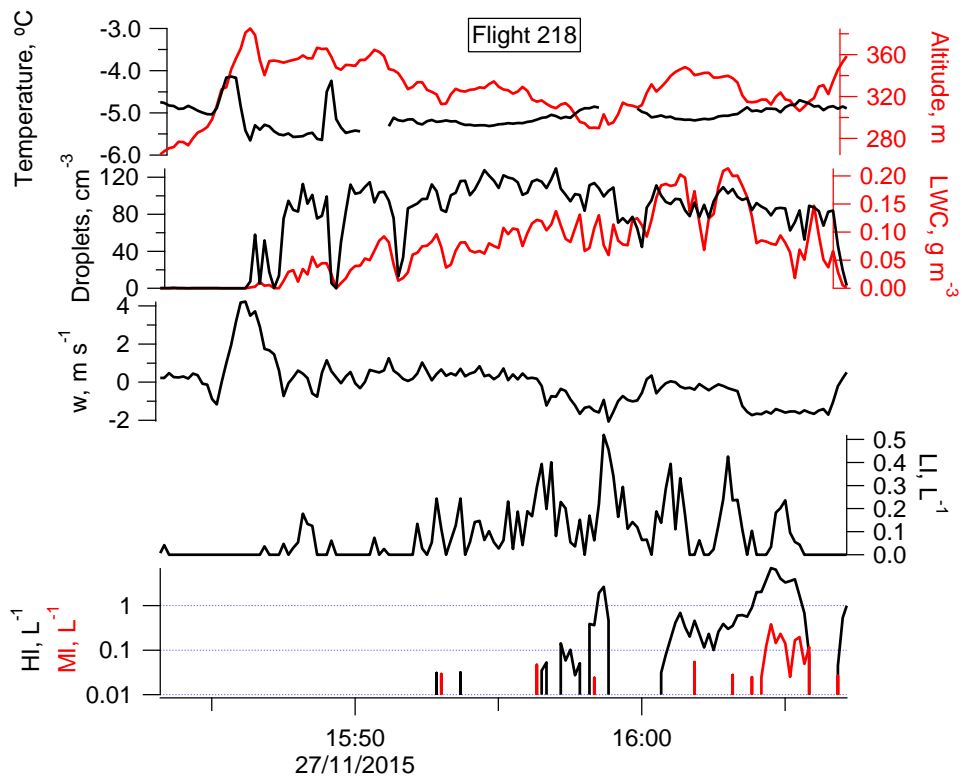


7

8 *Figure 7a. Comparison between the size distributions for 3 regions sampled in the constant*  
9 *altitude run at -5 °C during Flight 218, these are where the concentration of highly irregular*  
10 *particles (2DS HI) was  $7 \text{ L}^{-1}$  (4:04 GMT),  $3 \text{ L}^{-1}$  (3:58 GMT) and  $0 \text{ L}^{-1}$  (3:52 GMT). Time*  
11 *series of the microphysical measurements during this run are shown in Figure 8. Figure 7b*  
12 *shows a similar plot for a run at -6 °C during Flight 219 when the 2DS highly irregular*  
13 *concentration was  $50 \text{ L}^{-1}$ ,  $1 \text{ L}^{-1}$  and  $0 \text{ L}^{-1}$ .*



1



2

GMT

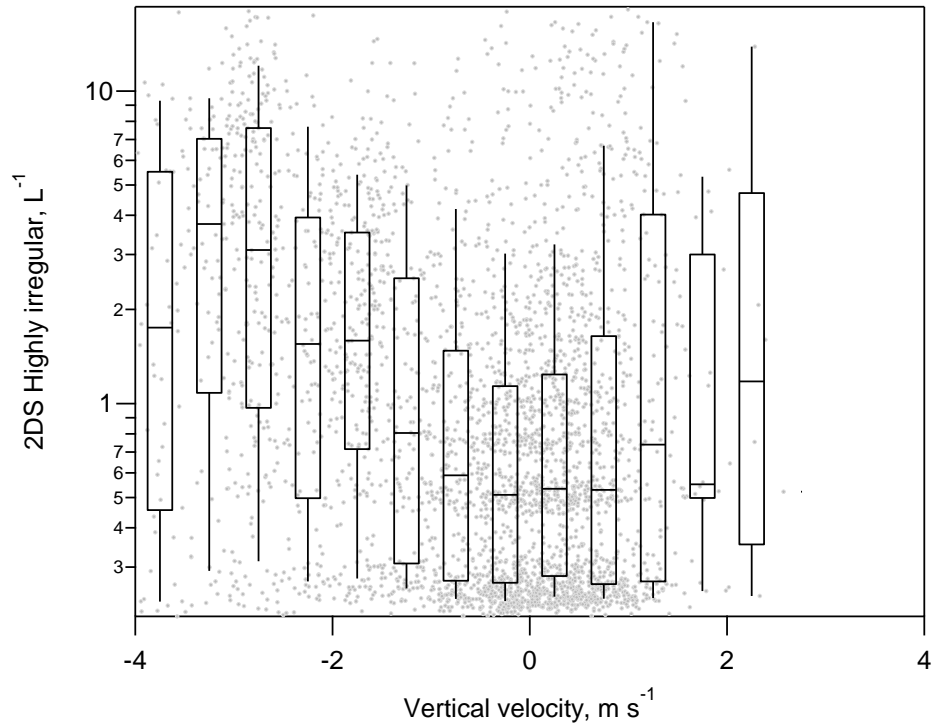
3 *Figure 8. Time series of microphysical parameters during a constant altitude run at -5°C*  
4 *(400 m) during flight 218.*

5

6 During MAC there was a trend towards higher ice concentrations in both updrafts and  
7 downdrafts compared to quiescent regions of the clouds (see Fig. 9 for measurements during  
8 constant altitude runs). Previous measurements have observed secondary ice production in  
9 convective regions of mid-latitude stratus (Crosier et al., 2011). The run during Flight 218 at -  
10 5 °C (see Fig. 8) is an example of this where the two peaks at 3:58 (2DS HI maximum = 3 L⁻  
11 <sup>1</sup>) and 4:04 (2DS HI maximum = 7 L⁻<sup>1</sup>) in ice concentration occur in downdrafts of  
12 approximately 1 m s⁻<sup>1</sup>. In contrast a similar run during Flight 219 (Fig. 7b) showed glaciated  
13 regions not to be associated with vertical motion.



1



2

3 *Figure 9. Box and whisker plots summarising the 1 Hz concentration of highly irregular*  
4 *particles (2DS HI) as a function of vertical velocity. Higher concentrations are observed in*  
5 *updrafts/downdrafts compared to quiescent regions.*

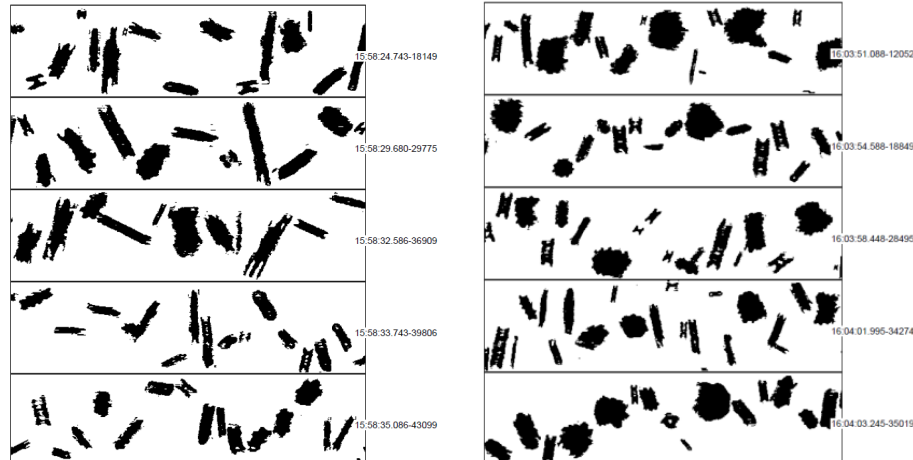
6

7 Inspection of the cloud particle images shows that at temperatures higher than  $-10^{\circ}\text{C}$   
8 columnar crystals appear as the dominant ice crystal habit, with irregular rimed crystals also  
9 widespread. This is illustrated by Fig. 10a showing example images from Flight 218 at  $-5^{\circ}\text{C}$ .  
10 Measurements in Arctic clouds at similar temperatures show that they are similarly dominated  
11 by columnar crystals (Lloyd et al., 2015a). Figure 10b. shows images at  $-15^{\circ}\text{C}$  collected in a  
12 single layer cloud over the Antarctic continent, approximately 300 km south of Halley (Flight  
13 233). This cloud had some columns/needles, but also a high proportion of plates and stellar  
14 crystals. At the lowest sampled temperatures of  $-20^{\circ}\text{C}$  (Fig. 10c, Flight 226) the ice mostly  
15 consists of rosettes and irregular crystals, which may be aggregates. However, measurements



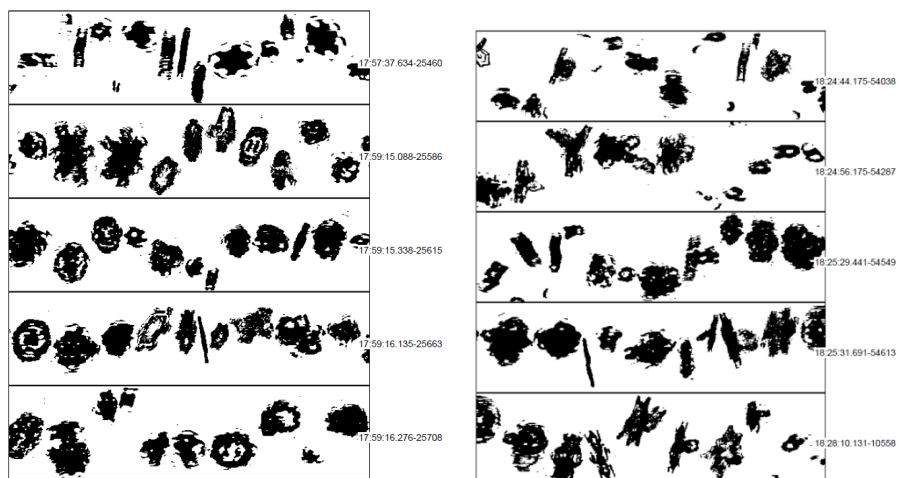
1 at these low temperatures were relatively infrequent, and the ice may have been nucleated at  
2 lower temperatures higher in the cloud.

3



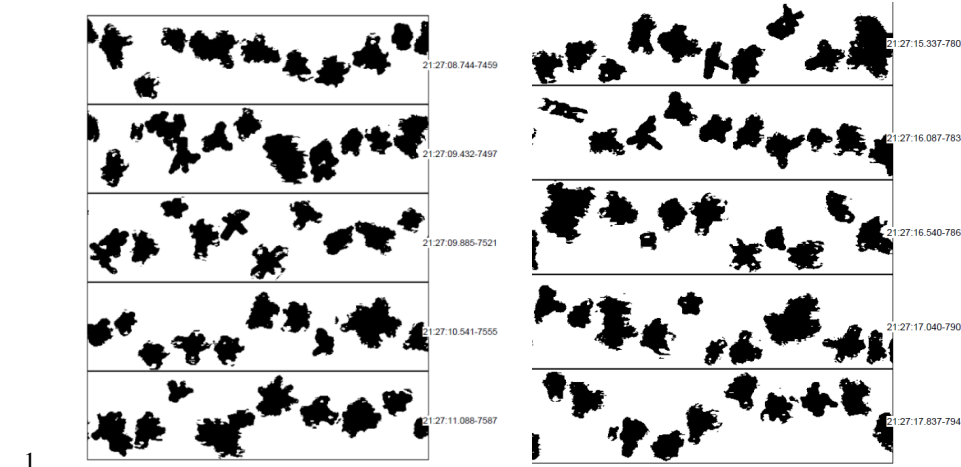
5 *Figure 10a. 2DS Images of highly irregular particles during a constant altitude run at -5°C  
6 (400 m) during flight 218.*

7



9 *Figure 10b. 2DS Images of highly irregular particles during a constant altitude run at -15°C  
10 during flight 233.*

11



1  
2 *Figure 10c. 2DS Images of highly irregular particles during a constant altitude run at -20°C*  
3 *during flight 226.*

4

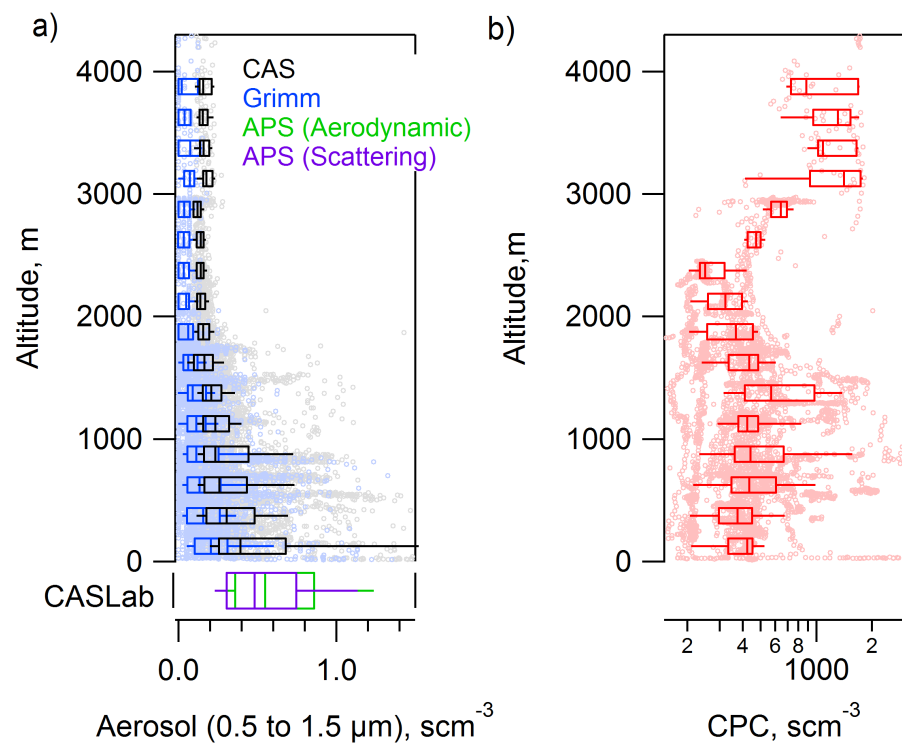
5 **3.2 Aerosol**

6 Vertical profiles of the out-of-cloud aerosol measurements made by the aircraft are shown in  
7 Fig. 11. Out-of-cloud measurements were selected as periods when the LWC was less than  
8  $0.001 \text{ g m}^{-3}$  and when the 2DS was not detecting particles. Contributions from large, swollen  
9 aerosol particles were also removed when the relative humidity was higher than 90%.  
10 Figure 11a shows aerosol concentrations over the size range from 0.5 to 1.5  $\mu\text{m}$  as observed  
11 by the CAS and GRIMM probes. This size range of aerosols has been shown to best represent  
12 the concentration of INPs in many locations around the world (DeMott et al., 2010).  
13 Concentrations within this size range decrease significantly with increasing height, as would  
14 be expected, through sea spray aerosol being rapidly removed by cloud processing or  
15 sedimentation. Total aerosol concentrations, measured by the CPC, had a median value for the  
16 campaign of  $408 \text{ cm}^{-3}$  and an inter-quartile range of  $260 \text{ cm}^{-3}$ .  
17 Previous, multi-year measurements of aerosol at the Neumayer coastal Antarctic research  
18 station had a median concentration of  $258 \text{ cm}^{-3}$ . Minimum values (less than  $100 \text{ cm}^{-3}$ ) were  
19 typically observed in June/July, while concentrations increased in the austral summer to a  
20 maximum of approximately  $1000 \text{ cm}^{-3}$  in March (Weller et al., 2011). In winter, aerosol  
21 number and mass were both dominated by sea salt particles (87% by mass, Weller et al.,



1 2008). Although aerosol composition in summer is more variable, sea salt still accounts for a  
2 significant fraction (50% by mass) but now with a large contribution from non sea salt  
3 sulphate (27% by mass, Weller et al., 2008). Measurements at the coastal Antarctic station  
4 McMurdo show the persistent presence of sulphate aerosol throughout the year (Giordano et  
5 al., 2017). In the winter these particles are highly aged. Sulphate aerosol then increases  
6 through the austral spring/summer, due to enhanced emissions of dimethyl sulphide (DMS)  
7 and methanesulfonic acid (MSA) from phytoplankton in the Southern Ocean (Gibson et al.,  
8 1990; Giordano et al., 2017). Giordano et al. (2017) also report the presence of a sub-250 nm  
9 aerosol population of unknown composition during the winter to summer transition. In  
10 addition a study has observed a significant fraction of organic carbon (>10%) and lower  
11 contributions from sea salt (<10%) in summer marine Antarctic aerosol (Virkkula and Teinil,  
12 2006).

13



14

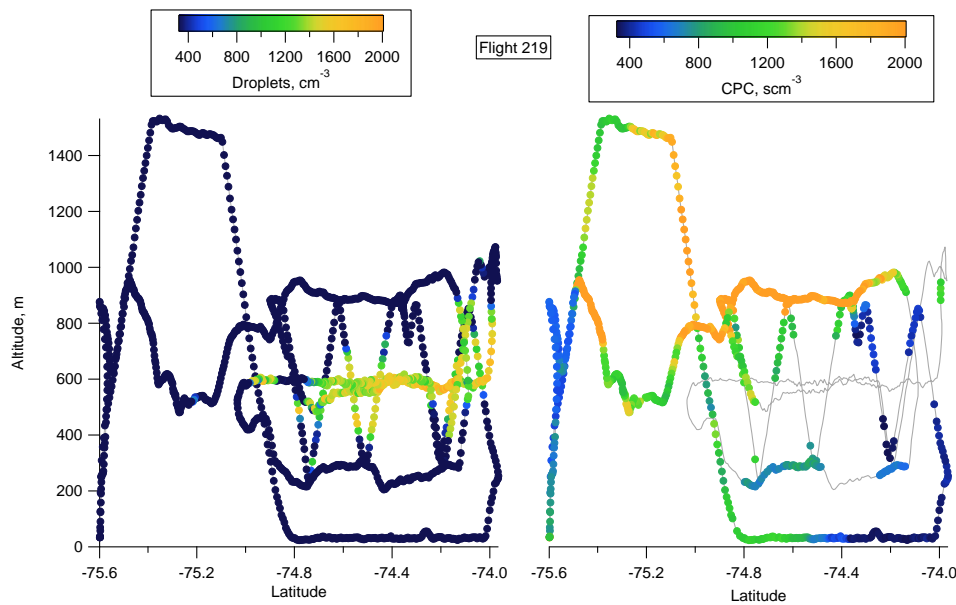
15 *Figure 11. Aircraft clear sky aerosol concentrations ( $\text{scm}^{-3}$ ) altitude profiles. Data are from:*  
16 *a) CAS and GRIMM instruments. Surface concentrations from CASLab are shown for*



1 comparison, from the APS; Green - aerodynamic particle size concentrations; Purple –  
2 scattering cross section derived particle size concentration measurements; b) Total fine  
3 aerosol concentration profiles, from CPC, ( $D > 10$  nm).

4

5 During MAC episodic periods were observed with total aerosol concentrations in excess of  
6  $1000 \text{ scm}^{-3}$ . These were often observed above cloud layers. The flights were designed to focus  
7 on cloud regions so may not represent a truly unbiased sample of the atmosphere, but the  
8 results do suggest a link between the observations of high aerosol concentrations and the  
9 presence of clouds. The limited spatial coverage of the aircraft measurements makes  
10 quantifying the extent of these layers uncertain, however they appear to extend over a few  
11 tens of kilometres to a hundred kilometres. At least two instances (flights 218, 219, see Fig.  
12 12) suggest a large layer extending beyond the cloud edge, pointing at the possibility of layers  
13 independent from clouds. The peak concentration usually occurred in the region up to 200 m  
14 above the cloud top (e.g. Flight 219). Some layers showed a clear drop in relative humidity  
15 (e.g. from 90% to 30%, e.g. during flight 220, 221, and 222) generally related to a clear  
16 temperature inversion, while other layers showed a much smaller decrease (by 10%) in  
17 relative humidity compared to the cloud underneath (e.g. flight 217, 218, 219). No clear  
18 systematic relationship was observed with respect to the vertical wind velocity (turbulence).  
19 The role of these particles as CCN/INPs is currently uncertain due to the lack of information  
20 about their composition.



1

2 *Figure 12. Latitudinal cross-sections of Flight 219 coloured by droplet concentration (left*  
3 *panel) and total aerosol concentrations out of cloud (right panel). Grey lines shows the flight*  
4 *track. These show a layer of high aerosol concentrations above the cloud top.*

5

6 Average total concentrations of UV-fluorescent aerosols (measured at CASLab with the  
7 WIBS) over the campaign period were  $\sim 1 \text{ L}^{-1}$ , which was  $< 2\%$  of the total particle  
8 concentration. Of these  $0.01 \text{ L}^{-1}$  were identified as likely primary biological aerosols using the  
9 analysis described by Crawford et al. (2015). During some Easterly and Westerly wind  
10 events, however, enhanced concentrations of the order of  $5\pm7 \text{ L}^{-1}$  could be observed.

11

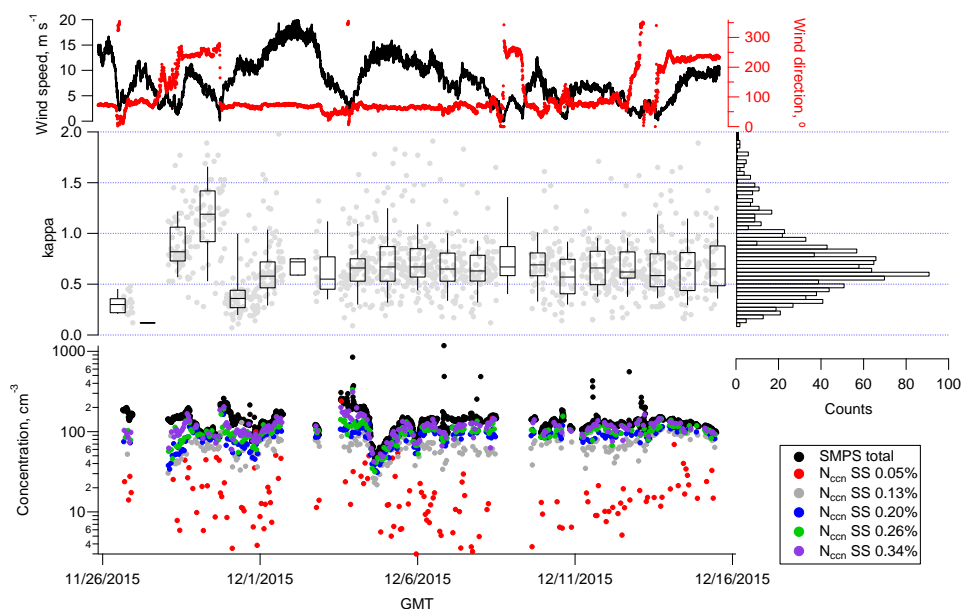
### 12 **3.3 Cloud condensation nuclei (CCN)**

13 Figure 13 (bottom panel) summarises the CCN measurements at the CASLab. The bottom  
14 panel shows the CCN at 5 different super saturations (0.05%, 0.13%, 0.20%, 0.26% and  
15 0.34%). The hygroscopicity parameter  $\kappa$  is used to examine the effect chemical composition  
16 has on the CCN activity of aerosol particles. The derived  $\kappa$  values represent the average  
17 hygroscopicity of the volume-weighted fractions of the individual aerosol components. Non-  
18 hygroscopic components have a  $\kappa$  value of 0. Highly CCN active salts have  $\kappa$  values between



1    0.5 and 1.4, sodium chloride (NaCl) has a  $\kappa$  of 1.28 (measurement range 0.91 to 1.33).  
2    Organic species have values generally between 0.01 and 0.5 (Petters and Kreidenweis, 2007).  
3    The median  $\kappa$  value during MAC was 0.64 (inter-quartile range = 0.34, mean = 0.69),  
4    suggesting that this location is dominated by hygroscopic components, such as sea-salt and  
5    sulphate. Andreae and Rosenfeld (2008) review CCN measurements and find that  $\kappa$  values  
6    from marine locations generally cover a relatively narrow range of  $0.7 \pm 0.2$ , compared to  $0.3$   
7     $\pm 0.1$  for continental aerosols. A global model study subsequently presented a mean  $\kappa$  value of  
8    0.92 (0.09 at  $1\sigma$ ) at the surface and 0.80 (0.17 at  $1\sigma$ ) within the boundary layer over the  
9    Southern Ocean (Pringle et al., 2010), only marginally higher than our MAC observations.

10



11

12    *Figure 13. The top panel shows the time series of wind speed (black line) and direction (red  
13    markers) at the CASLab. The middle panel shows the time series of the hygroscopicity  
14    parameter  $\kappa$ . The box and whisker plots summarise the variability in  $\kappa$  for each day, while the  
15    right panel shows a histogram of  $\kappa$  for the whole measurement period. The bottom panel  
16    shows the total aerosol number from the integrated SMPS measurements (30 to 500 nm, black  
17    dots) and the CCN concentrations at 5 different supersaturations (SS, coloured dots from 0.05  
18    to 0.34%).*

19



1 As shown in Fig. 13 there was a period of increased hygroscopicity on 28 and 29 November  
2 2015, with a median  $\kappa$  of 1.18 on 29 November. During this period there was a westerly wind.  
3 This changed to an easterly on 30 November 2015, which coincided with a decrease in  
4 hygroscopicity to a median  $\kappa$  for the 30 November of 0.36. Between the approximate  
5 headings  $210^\circ$  to  $25^\circ$  the CASLab lies between 30 and 60 km from the Weddell Sea. In  
6 contrast, within the sector  $30^\circ$  to  $60^\circ$  it lies several hundred km across the Brunt Ice Shelf  
7 from the Weddell Sea. To the south east of the CASLab lies the Antarctic Continent.  
8 However after 30 November 2015 the hygroscopicity was relatively consistent and does not  
9 show a significant relationship with the wind direction. For example, on the 14 and 15  
10 December 2015 there was a westerly wind but the median  $\kappa$  for these days of 0.66 and 0.65,  
11 respectively, was similar to the campaign median (0.64).

12 **3.4 Ice nucleating particles (INPs)**

13 Ice nucleating particles (INPs) could not be directly measured on the aircraft during MAC.  
14 Instead we compare the cloud ice crystal concentrations with two parameterisations that are  
15 commonly used to predict INP concentrations. DeMott et al. (2010) compiled INP  
16 measurements from a range of locations around the world and derived a relationship using  
17 aerosol concentrations (within the size range 0.5 to 1.6  $\mu\text{m}$ ) and temperature that could  
18 explain the INP variability within their dataset to better than a factor of 10. For a broad  
19 comparison with the MAC dataset we evaluate DeMott et al. (2010) for a high ( $1 \text{ scm}^{-3}$ , dark  
20 blue lines, Fig. 5b) and low ( $0.1 \text{ scm}^{-3}$ , light blue lines, Fig. 5b) aerosol case. Cooper (1986)  
21 describes a simple INP parameterisation using only the ambient temperature, which is often  
22 used in the Weather Research Forecasting model (WRF) (Morrison et al., 2009). The  
23 concentration of INPs from Cooper (1986) is shown as a red line in Fig. 5b. It should be noted  
24 that neither of these parameterisations use Antarctic measurements. Given the marine location  
25 of the flights it is likely that these parameterisations may represent overestimates of the true  
26 INP concentration, since the number of INP in sea spray aerosol is generally several orders of  
27 magnitude lower than the number of INP in aerosol in the continental boundary layer (DeMott  
28 et al., 2015). The DeMott et al. (2010) parameterisation was derived using measurements at  
29 temperatures lower than  $-9^\circ\text{C}$ , while Cooper (1986) used measurements below  $-5^\circ\text{C}$ . For  
30 comparison they are extrapolated to higher temperatures and are therefore subject to increased  
31 uncertainty.



As shown in Fig. 5b, given the uncertainty in both parameterisations and the challenges with making a direct comparison with the measurements it is plausible that the observed ice concentrations at temperatures lower than ca -10 °C could be explained by primary ice production. However above this temperature the measured ice concentrations diverge from the predicted INP by 1 to 3 orders of magnitude, suggesting that secondary ice production is becoming increasingly dominant.

Below -9 °C, where secondary ice production is likely to be less significant, Listowski and Lachlan-Cope (2017) found that the number of INP predicted by DeMott et al. (2010) gave better agreement with observed ice concentrations over the Antarctic Peninsula compared to INP parameterisations that only use the ambient temperature as input. For MAC, each in cloud data point was compared with the closest (in time) out-of-cloud aerosol measurement (1 minute average, RH < 90%). Data points were excluded from the comparison if no out-of-cloud aerosol measurements were made within 10 minutes of the in-cloud measurement. No clear relationship was found between the local aerosol concentrations and the ice concentrations ( $R^2=0.02$  for the above cloud aerosol in the size range 0.5 to 1.6  $\mu\text{m}$ ). During MAC, the majority of cloud measurements showed no ice (see Fig. 3) suggesting that the Antarctic is a very low INP environment. As a result, all conventional INP schemes will likely overestimate the true concentrations.

19

### 20 **3.5 Airmass history**

To examine how aerosol and cloud properties vary with airmass history we perform back trajectory analysis using the UK Met. Office's NAME model (Numerical Atmospheric Dispersion Modelling Environment) (Jones et al., 2007) using Met Office Unified Model (UM) meteorological fields. Five-day retroplumes were determined by releasing 10000 particles in the model at locations coincident with the aircraft's position. Here we examine the relative sensitivity to surface emissions from the following regions; the Antarctic continent, sea ice, Southern Ocean, ice-shelf and South America. The numbers of particles near the surface (0 to 100 m) over each geographic region was summed every 15 minutes as the particles were dispersed five-days backwards in time. For each region, the time integration of particles over the region was divided by the total number of particles appearing in the whole domain to determine fractional contributions (see Fleming et al., 2012). Shape files

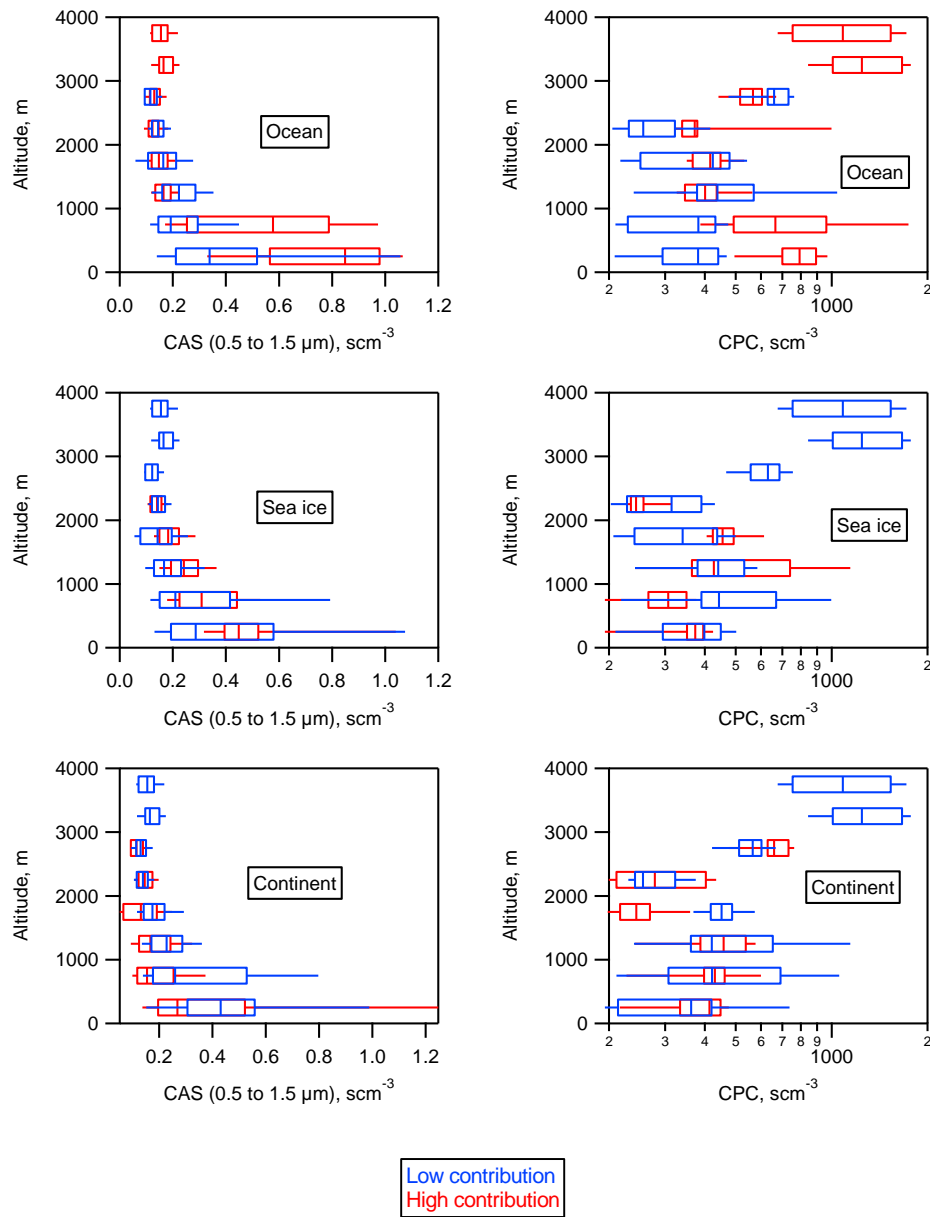


1 representing the monthly averaged sea ice extent from Polarview and geographical contour  
2 files for the Antarctic plateau, the permanent sea ice (ice shelves and permanent sea ice) and  
3 the American continent were used to determine the passageway of the air masses at surface  
4 levels sampled by the aircraft. This analysis was repeated for particles released at 60s  
5 intervals along the flight track to determine a time series of contributions from each  
6 geographic region.

7 Figure 14 shows vertical profiles of the aerosol from the CAS (0.5 to 1.5  $\mu\text{m}$ , relative  
8 humidity < 90%) when there was high (>50%, red markers) and low (<50%, blue markers)  
9 surface influence from the Southern Ocean, the sea ice and the Antarctic Continent. There is a  
10 broad trend of higher aerosol concentrations over this size range with greater contributions  
11 from the Ocean and sea ice, indicating significant emissions of sea salt/sulphate aerosol.  
12 Concentrations decrease with increased contributions from the continent, indicating a lack of  
13 sources in this region. These relationships are more distinct when the aircraft was sampling at  
14 low altitude, above approximately 1000 m the concentrations are less dependent on airmass  
15 origin due to their lower surface influence. This analysis was repeated using total aerosol  
16 concentrations from the CPC (Fig. 14). Similar to the CAS, higher concentrations were  
17 observed when there was greater influence from the Southern Ocean, with the differences  
18 again most distinct for the low altitude measurements. However, CPC concentrations are  
19 found to be less dependent on the influence of the sea ice and the Antarctic Continent.

20

21



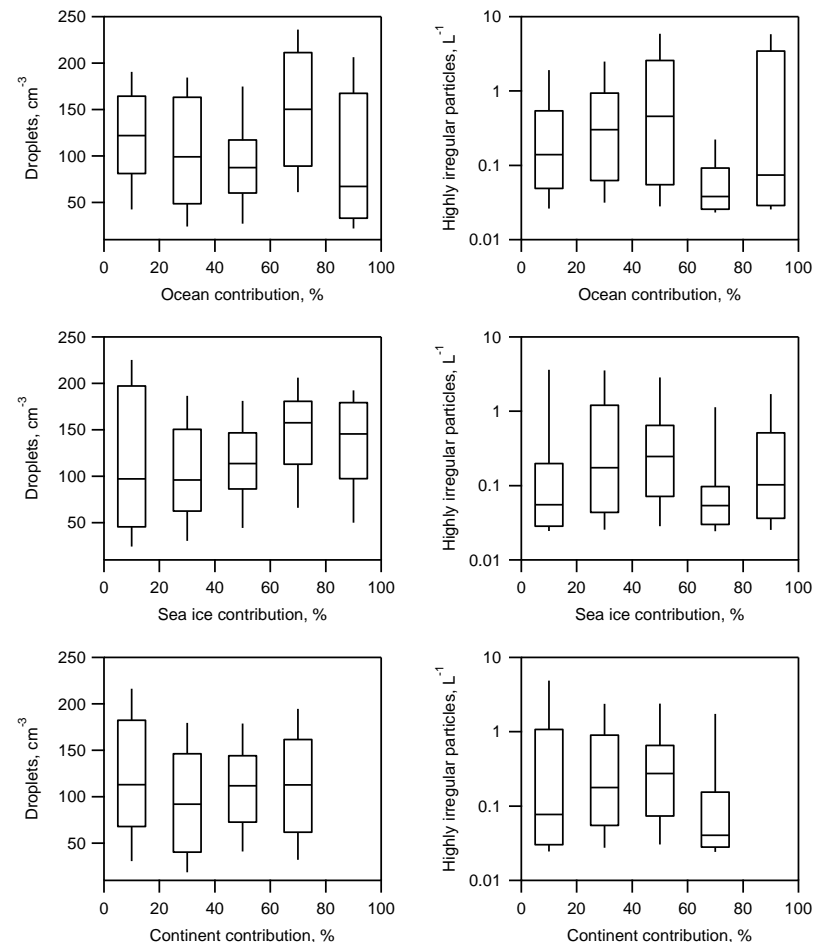
1  
 2 *Figure 14. Altitude profiles of CAS aerosol over the size range 0.5 to 1.5  $\mu\text{m}$  (left panels) and*  
 3 *total aerosol, greater than 10nm from the CPC (right panels). The measurements have been*  
 4 *partitioned into periods when the airmass had a high (red) and low (blue) contributions from*  
 5 *different geographic regions (see text for details).*



1

2 Compared to the aerosol measurements the concentrations of cloud droplets and 2DS irregular  
3 particles are found to be less dependent on airmass history. Figure 15 shows these variables as  
4 a function of the relative surface influence from the Southern Ocean, sea ice and the  
5 continent. The concentration of ice in the clouds is found to decrease for airmasses with  
6 increasing influence from the ocean. However, due to ice in the clouds being relatively  
7 infrequently observed the significance of this relationship cannot be determined. The effects  
8 of airmass history cannot easily be deconvolved from differences in sampling strategy or  
9 cloud properties (e.g. humidity, temperature, dynamics, and secondary ice production). Most  
10 of the flights were conducted over sea ice, meaning that near field influences may be  
11 obscuring any relationship with airmass origin.

12



1  
2 *Figure 15. The concentration of cloud droplets and 2DS highly irregular particles as function*  
3 *of the air mass's contribution from the Southern Ocean, sea ice and the continent (see text for*  
4 *details). Boxes give the 25<sup>th</sup> and 75<sup>th</sup> and the whiskers are the 10<sup>th</sup> and 90<sup>th</sup> percentiles for*  
5 *each regional contribution bin.*

6

#### 7 **4 Discussion**

8 Ice in the clouds exhibited a high degree of variability, occurring in small patches. Constant  
9 altitude runs by the aircraft through clouds at slightly supercooled temperatures ( $> -10^{\circ}\text{C}$ )  
10 showed ice-free regions with patches of high ice concentrations ( $> 1 \text{ L}^{-1}$ ). This variability is  
11 shown to exist over small spatial scales and may be a consequence of very low INP



1 concentrations, where secondary processes may significantly amplify small differences in INP  
2 concentrations. This makes predicting in detail where ice will form in a given cloud extremely  
3 challenging. A detailed understanding of where the first ice will occur and also the conditions  
4 required for secondary production is needed. Here we examine this variability and discuss  
5 some of the potential controlling factors.

6

#### 7 **4.1 First Ice**

8 First we examine the nature and sources of the INP. Global primary ice nucleation below  
9 approximately -15°C is thought to be dominated by soot and mineral dusts (Möhler et al.,  
10 2006; Murray et al., 2012; Niemand et al., 2012). However, this is colder than the cloud top  
11 temperatures generally observed during MAC. Biological species (pollen, bacteria, fungal  
12 spores and plankton) are the only INP that are known to be active at temperatures higher than  
13 approximately -15°C (Alpert et al., 2011; Murray et al., 2012; Wilson et al., 2015). Bioaerosol  
14 measurements at the CASLab show episodic high concentrations up to several per litre. This  
15 temporal variability in bioaerosol may be analogous to the spatial variability of the ice  
16 crystals observed in the clouds. Source apportionment of the bioaerosol at Halley is uncertain  
17 with the available dataset, but may include contributions from 1) the re-suspension of material  
18 from the local ice and snow surface, 2) coastal ice margin zones in Halley Bay where bird  
19 colonies are present and 3) long-range transport. The bioaerosol measurements will be  
20 presented and discussed in detail in a separate paper.

21 It is possible that the cloud layers sampled in MAC are seeded by precipitation from higher  
22 layers where the temperatures are low enough for dust to be active as an INP. During MAC  
23 the flights were designed so that measurements were performed between cloud layers to  
24 determine whether ice seeding from the upper layers was occurring. The frontal cloud  
25 sampled in flight 224 showed extensive ice precipitating between cloud layers and the cloud  
26 top temperature (below -20 °C) was sufficiently low for dust to be a potential source of ice  
27 nuclei. In the case of stratus clouds, those were not found to be seeded by layers at low  
28 enough temperatures for any dust to be active as an INP. Furthermore, single layer clouds  
29 such as those sampled in flights 219 and 227 still showed the patchy ice behaviour.

30 Detailed measurements of aerosol composition were not available on the aircraft. No clear  
31 relationship could be identified between the local aerosol concentrations and the presence of



ice in the clouds. However, only a small proportion of the total aerosol population are expected to be INP. Below ca 2000 m (where most of MAC measurements were performed) there is a broad trend of ice being more frequent with decreasing altitude. A similar relationship is observed for the concentration of particles between 0.5 and 1.6  $\mu\text{m}$  (Fig. 4). However, this may in part be due to secondary ice production being efficient at these relatively high temperatures. Jackson et al. (2012) found a correlation ( $R=0.69$ ) between the above cloud aerosol ( $0.1 < D < 3 \mu\text{m}$ ) and ice concentrations in Arctic stratocumulus clouds. However these clouds were generally at lower temperatures (cloud top temperature  $< -10^\circ\text{C}$ ) than those during MAC and as a result are likely to have a higher proportion of primary ice production.

The surface may also be an ice crystal source either through blowing snow (Ardon-Dryer et al., 2011) or frost flowers (Gallet et al., 2014; Lloyd et al., 2015b). These will be most important for clouds in contact with the surface (Vali et al., 2012), but may also be relevant for low clouds when the humidity is sufficiently high that the crystals do not evaporate whilst being transported to the cloud base (Geerts et al., 2015). Space-borne lidar measurements of blowing snow over Antarctica found the thickness of these layers ranging between their detection limit (30 m) up to 1000 m, with an average thickness of 100 m. Approximately 71% of these layers were less than 100 m thick and 25% were between 100 and 300 m thick (Palm et al., 2011). Similarly, lidar measurements at the South Pole found that layers were generally less than 400 m thick (63%), but could be up to 1000 m thick. Blowing snow is almost always constrained to the planetary boundary layer (Mahesh, 2003). The lofting of snow is complex; it is dependent on a range of variables, including: the snow type and surface meteorology (e.g. wind speed, turbulent mixing, temperature and humidity). A threshold wind speed of 7 to 10  $\text{m s}^{-1}$  is typically required (Dery and Yau, 1999). However, smaller crystals may show substantial fluxes at lower wind speeds. Aerosol fluxes from evaporated frost flowers have been estimated at  $10^{-6} \text{ m}^{-2} \text{ s}^{-1}$  at wind speeds as low as  $1 \text{ m s}^{-1}$  (Xu et al., 2013).

Evaluating the impact of these mechanisms during MAC is challenging since most of the in-cloud sampling was performed over snow covered sea ice, making it difficult to attribute local differences in the microphysics to the surface type. Flight 218 (Fig. 8) is one case where the first ice development may be due to surface ice crystals. During this flight ice was observed precipitating below cloud base. The majority of this ice precipitation was detected when flying over snow covered sea ice rather than open water. This was identified from the



1 aircraft's forward facing camera and inspection of the surface albedo. Given the relatively low  
2 cloud base (300m), strong surface horizontal winds (5 to 10 m s<sup>-1</sup>) and a relative humidity  
3 approaching 100% it is plausible that ice from the surface (e.g. from blowing snow) could  
4 mix up to cloud base, thus providing the first ice to the cloud. The sublimation rate of an ice  
5 crystal is largely dependent on the humidity. A 100 µm ice crystal at 0°C will have a lifetime  
6 of the order 100s at a relative humidity of 80%. At relative humidities of 90% and 95% the  
7 lifetime can be over 200 s and 400 s, respectively (Thorpe and Mason, 1966). The ice crystals  
8 below cloud had similar habits to those observed in the cloud (a mixture of columns and  
9 rimed crystals) indicating they had not originated from the surface. However, only low  
10 concentrations of primary ice from the surface is needed if the ice is then able to multiply  
11 within the cloud due to secondary processes.

12

#### 13 **4.2 Secondary Ice**

14 Previous ice crystal observations over the Antarctic Peninsula show a similar behaviour to  
15 those during MAC with a peak in ice concentrations (> 1 L<sup>-1</sup>) at approximately -5°C.  
16 Grosvenor et al. (2012) and Lachlan-Cope et al. (2016) attribute this to secondary ice  
17 production through the Hallett-Mossop process, where ice splinters are produced when a  
18 droplet freezes subsequent to colliding with an ice crystal (riming) (Hallett and Mossop,  
19 1974). This can lead to rapid ice multiplication as the splinters freeze further drops, resulting  
20 in more splinters. Laboratory experiments suggest that this process is efficient over a narrow  
21 temperature range (-8 to -3 °C) with a peak at -5 °C (Mossop, 1976). Images from the 2DS  
22 probe at temperatures higher than -10°C generally show rimed crystals and small columns  
23 (Fig. 10a). These habits are generally observed when the Hallett-Mossop production  
24 mechanism is thought to be occurring (Crosier et al., 2011; Lloyd et al., 2015a).

25 A number of other secondary ice mechanisms have previously been identified, these include:  
26 large drops producing ice splinters when they freeze (Lawson et al., 2015); and the break-up  
27 of ice crystals, generally either fragile dendrites due to sublimation, turbulence (Bacon et al.,  
28 1998) or because of collisions between crystals (Yano and Phillips, 2011). However, all these  
29 processes have only been observed to be efficient at temperatures lower than approximately -  
30 10 °C, which is lower than the temperature of the majority of clouds sampled during MAC.  
31 Taylor et al. (2015) suggest that the drop-freezing secondary ice production, identified by



1 Lawson et al. (2015), may have occurred at temperatures higher than -10 °C in their  
2 measurements of cumulus clouds. However, they were not able to deconvolve its effects from  
3 the Hallett-Mossop mechanism. We have not performed automatic habit recognition on the  
4 2DS images taken during MAC, however, inspecting the images “by-eye” suggests that the  
5 drop shattering events observed by Lawson et al. (2015) were not common during MAC.

6 The exact requirements for secondary ice production through Hallett-Mossop are still  
7 uncertain. It is thought that only a small amount of primary ice is needed for it to be  
8 initiated, and recent model studies suggest this could be as low as 0.01 L<sup>-1</sup> (Crawford et al.,  
9 2012; Huang et al., 2017). Laboratory experiments suggest that production rates are  
10 proportional to the accumulation of large drops (>24 µm) (Mossop and Hallett, 1974).  
11 However, more recent field measurements found that estimated crystal production rates gave  
12 better agreement with observed ice concentrations if this constraint on drop diameter was  
13 removed (Crosier et al., 2011). Observations of Arctic mixed phase clouds found that the  
14 presence of precipitating ice particles (> 400 µm) was correlated with the number of large  
15 drops (>30 µm), however the precise nucleation mechanism through which this occurred was  
16 uncertain (Lance et al., 2011). During MAC both the analysis of individual case studies and  
17 the statistics for the whole campaign do not suggest that the concentration of large drops and  
18 ice crystals were related. However, any simple relationship is likely to be complicated as ice  
19 crystal growth will deplete the drops through riming and the Wegener-Bergeron-Findeisen  
20 process. This is shown in Fig. 6 and 7b where the highest ice concentrations correspond to  
21 relatively low droplet concentrations.

22 Flights 226, 227 and 228 involved sequential vertical profiles to examine the dependency of  
23 ice on the clouds vertical structure. No link was identified between the presence of ice in the  
24 vertical profile and local variations in cloud top temperature. However, since the first ice  
25 occurs over small spatial scales, any relationship may be obscured by the aircraft’s horizontal  
26 motion whilst changing altitude. As a result the precise cloud top temperature, and its  
27 variability, directly above the glaciated regions of the clouds is not known.

28 Higher ice concentrations were observed in updrafts/downdrafts compared to quiescent  
29 regions of the clouds. There are several possible explanations for this; first the more turbulent  
30 conditions may make more primary ice available through greater entrainment of aerosol and  
31 hence potentially more INP into the cloud. Second convective regions may indicate thicker  
32 regions of the cloud and lower cloud top temperature. This may lead to increased primary ice



1 nucleation as the lower temperatures activate more INPs and the development of larger liquid  
2 droplets. Third, the more turbulent conditions could lead to more efficient ice production due  
3 to ice being rapidly mixed to the Hallett-Mossop zone where concentrations would multiply.  
4 Finally, the riming rate may increase due to a greater number of ice-liquid collisions. More  
5 turbulent conditions may also indicate higher rimer velocity, however laboratory experiments  
6 suggest there is no lower cut-off rimer velocity for Hallett-Mossop to be active (Mossop,  
7 1985).

8

## 9 5 Conclusions

10 We have reported observations of cloud and aerosol properties over coastal Antarctica and the  
11 Weddell Sea. The aerosol was predominantly hygroscopic in nature, with  $\kappa$  being consistent  
12 with previous measurements and model predictions for remote locations dominated by marine  
13 emissions. The concentration of large aerosols (0.5 to 1.6  $\mu\text{m}$ ) decreased with altitude, as  
14 would be expected, through sea salt/sulphate aerosol being rapidly removed by cloud  
15 processing or sedimentation. Higher aerosol concentrations were observed in airmasses that  
16 travelled over the Southern Ocean/sea ice compared to those from the main Antarctic  
17 Continent.

18 In contrast to the aerosol concentrations, the droplet and ice concentrations showed minimal  
19 dependence on airmass origin. The cloud types were generally stratus, both single and  
20 multiple layers, at temperatures between -20 and -3 °C. These were dominated by super-  
21 cooled liquid drops, with a median concentration of  $113 \text{ cm}^{-3}$ . Droplet concentrations were  
22 relatively consistent throughout the campaign with an inter-quartile range of  $86 \text{ cm}^{-3}$ . The  
23 exceptions to this were cases when the concentrations became depleted by high ice  
24 concentrations, and also during Flight 217 when anomalously high droplet concentrations  
25 were observed; this was associated with an enhanced aerosol layer below the cloud layer.

26 Ice in the clouds exhibited a high degree of inhomogeneity occurring in small patches. Below  
27 ca 2000 m ice was more frequent at higher temperatures, however even within the -8 to -3 °C  
28 temperature range where Hallett-Mossop secondary production is most active, the clouds  
29 were predominantly liquid. When ice was present within the temperature range -8 to -3 °C it  
30 seems likely that secondary ice production, through the Hallett-Mossop process, resulted in  
31 concentrations that were 1 to 3 orders of magnitude higher than the number of INP predicted  
32 by conventional primary ice nucleation schemes. The source of first ice in the clouds is



1 currently uncertain. First ice in the clouds often occurs at temperatures above -10 °C, this may  
2 be due to the presence of biogenic particles that are active INP at these temperatures or  
3 alternatively (or indeed simultaneously) ice from the surface (e.g. blowing snow or frost  
4 flowers) could be lofted into the clouds. The drivers of the ice crystal variability were  
5 investigated. No dependence on the droplet spectrum was found. However, higher ice  
6 concentrations were found in updrafts and downdrafts compared to quiescent zones, and  
7 therefore intermittent convective activity may explain the intermittent glaciation of clouds.

8 This paper has presented the most detailed in situ observations of coastal Antarctic clouds and  
9 their surrounding aerosol properties to date. Upcoming studies will use the MAC observations  
10 to test and improve the representation of Antarctic clouds in numerical weather/climate  
11 models.

12

13 **Acknowledgements**

14 The authors would like to thank Vicky Auld and all the BAS staff who helped in the  
15 Antarctic. The MAC project was funded by the UK Natural Environment Research Council  
16 (Grant number: NE/K01482X/1).

17



## 1 References

- 2 Alpert, P. A., Aller, J. Y. and Knopf, D. A.: Initiation of the ice phase by marine biogenic  
3 surfaces in supersaturated gas and supercooled aqueous phases, *Phys. Chem. Chem. Phys.*,  
4 13(44), 19882, doi:10.1039/c1cp21844a, 2011.
- 5 Amato, P., Joly, M., Schaupp, C., Attard, E., Möhler, O., Morris, C. E., Brunet, Y. and Delort,  
6 A. M.: Survival and ice nucleation activity of bacteria as aerosols in a cloud simulation  
7 chamber, *Atmos. Chem. Phys.*, 15(11), 6455–6465, doi:10.5194/acp-15-6455-2015, 2015.
- 8 Andreae, M. O. and Rosenfeld, D.: Aerosol-cloud-precipitation interactions. Part 1. The  
9 nature and sources of cloud-active aerosols, *Earth-Science Rev.*, 89(1–2), 13–41,  
10 doi:10.1016/j.earscirev.2008.03.001, 2008.
- 11 Ardon-Dryer, K., Levin, Z. and Lawson, R. P.: Characteristics of immersion freezing nuclei at  
12 the South Pole station in Antarctica, , (2008), 4015–4024, doi:10.5194/acp-11-4015-2011,  
13 2011.
- 14 Bacon, N. J., Swanson, B. D., Baker, M. B. and Davis, E. J.: Breakup of levitated frost  
15 particles, *J. Geophys. Res.*, 103(D12), 13763–13775, doi:10.1029/98JD01162, 1998.
- 16 Baumgardner, D., Jonsson, H., Dawson, W., O'Connor, D. and Newton, R.: The cloud,  
17 aerosol and precipitation spectrometer: a new instrument for cloud investigations, *Atmos.*  
18 *Res.*, 59–60, 251–264, doi:10.1016/S0169-8095(01)00119-3, 2001.
- 19 Baumgardner, D., Newton, R., Krämer, M., Meyer, J., Beyer, A., Wendisch, M. and  
20 Vochezer, P.: The cloud particle spectrometer with polarization detection (CPSPD): A next  
21 generation open-path cloud probe for distinguishing liquid cloud droplets from ice crystals,  
22 *Atmos. Res.*, 142, 2–14, doi:10.1016/j.atmosres.2013.12.010, 2014.
- 23 Bigg, E. K.: Long-term trends in ice nucleus concentrations, *Atmos. Res.*, 25(5), 409–415,  
24 doi:10.1016/0169-8095(90)90025-8, 1990.
- 25 Bodas-Salcedo, A., Williams, K. D., Field, P. R. and Lock, A. P.: The surface downwelling  
26 solar radiation surplus over the southern ocean in the met office model: The role of  
27 midlatitude cyclone clouds, *J. Clim.*, 25(21), 7467–7486, doi:10.1175/JCLI-D-11-00702.1,  
28 2012.
- 29 Bodas-Salcedo, A., Hill, P. G., Furtado, K., Karmalkar, A., Williams, K. D., Field, P. R.,  
30 Manners, J. C., Hyder, P., and Kato, S.: Large contribution of supercooled liquid clouds to the



- 1 solar radiation budget of the Southern Ocean, *J. Climate*, 29, 4213–4228, 2016.
- 2 van den Broeke, M. R., Bamber, J., Lenaerts, J. and Rignot, E.: *Ice Sheets and Sea Level: Thinking Outside the Box*, *Surv. Geophys.*, 32(4–5), 495–505, doi:10.1007/s10712-011-9137-z, 2011.
- 3 Bromwich, D. H., Nicolas, J. P., Hines, K. M., Kay, J. E., Key, E. L., Lazzara, M. A., Lubin, D., McFarquhar, G. M., Gorodetskaya, I. V., Grosvenor, D. P., Lachlan-Cope, T. and Van Lipzig, N. P. M.: Tropospheric clouds in Antarctica, *Rev. Geophys.*, 50(1), 1–40, doi:10.1029/2011RG000363, 2012.
- 4 Bromwich, D. H., Otieno, F. O., Hines, K. M., Manning, K. W. and Shilo, E.: Comprehensive evaluation of polar weather research and forecasting model performance in the antarctic, *J. Geophys. Res. Atmos.*, 118(2), 274–292, doi:10.1029/2012JD018139, 2013.
- 5 Brown, P. and Francis, P.: Improved measurements of the ice water content in cirrus using a total-water probe, *J. Atmos. Ocean.*, 1995.
- 6 Cavalieri, D. J., Parkinson, C. L., Gloersen, P., and Zwally, H. J.: Sea Ice Concentrations from Nimbus-7 SMMR and DMSP SSM/I-SSMIS Passive Microwave Data, Version 1, Sea Ice Concentrations from Nimbus-7 SMMR, Boulder, CO, USA, NASA National Snow and Ice Data Center Distributed Active Archive Center, available at: doi:10.5067/8GQ8LZQVL0VL (last access: January 2017), 1996.
- 7 Christner, B. C., Morris, C. E., Foreman, C. M., Cai, R. and Sands, D. C.: Ubiquity of biological ice nucleators in snowfall., *Science*, 319(5867), 1214, doi:10.1126/science.1149757, 2008.
- 8 Cooper, W. A.: *Ice Initiation in Natural Clouds*, *Meteorol. Monogr.*, 21(43), 29–32, doi:10.1175/0065-9401-21.43.29, 1986.
- 9 Crawford, I., Bower, K. N., Choularton, T. W., Dearden, C., Crosier, J., Westbrook, C., Capes, G., Coe, H., Connolly, P. J., Dorsey, J. R., Gallagher, M. W., Williams, P., Trembath, J., Cui, Z. and Blyth, A.: Ice formation and development in aged, wintertime cumulus over the UK: observations and modelling, *Atmos. Chem. Phys.*, 12(11), 4963–4985, doi:10.5194/acp-12-4963-2012, 2012.
- 10 Crawford, I., Robinson, N. H., Flynn, M. J., Foot, V. E., Gallagher, M. W., Huffman, J. A., Stanley, W. R., and Kaye, P. H.: Characterisation of bioaerosol emissions from a Colorado



- 1 pine forest: results from the BEACHON-RoMBAS experiment, *Atmos. Chem. Phys.*, 14,  
2 8559–8578, doi:10.5194/acp-14-8559-2014, 2014.
- 3 Crawford, I., et al. Evaluation of hierarchical agglomerative cluster analysis methods for  
4 discrimination of primary biological aerosol. *Atmos. Meas. Tech.*, 8, 4979–4991,  
5 doi:10.5194/amt-8-4979-2015, 2015.
- 6 Crosier, J., Bower, K. N., Choularton, T. W., Westbrook, C. D., Connolly, P. J., Cui, Z. Q.,  
7 Crawford, I. P., Capes, G. L., Coe, H., Dorsey, J. R., Williams, P. I., Illingworth, A. J.,  
8 Gallagher, M. W. and Blyth, A. M.: Observations of ice multiplication in a weakly  
9 convective cell embedded in supercooled mid-level stratus, *Atmos. Chem. Phys.*, 11(1), 257–  
10 273, doi:10.5194/acp-11-257-2011, 2011.
- 11 DeMott, P. J., Prenni, A. J., Liu, X., Kreidenweis, S. M., Petters, M. D., Twohy, C. H.,  
12 Richardson, M. S., Eidhammer, T. and Rogers, D. C.: Predicting global atmospheric ice  
13 nuclei distributions and their impacts on climate., *Proc. Natl. Acad. Sci. U. S. A.*, 107(25),  
14 11217–22, doi:10.1073/pnas.0910818107, 2010.
- 15 DeMott, P. J., Hill, T. C. J., McCluskey, C. S., Prather, K. A., Collins, D. B., Sullivan, R. C.,  
16 Ruppel, M. J., Mason, R. H., Irish, V. E., Lee, T., Hwang, C. Y., Rhee, T. S., Snider, J. R.,  
17 McMeeking, G. R., Dhaniyala, S., Lewis, E. R., Wentzell, J. J. B., Abbatt, J., Lee, C., Sultana,  
18 C. M., Ault, A. P., Axson, J. L., Diaz Martinez, M., Venero, I., Santos-Figueroa, G., Stokes,  
19 M. D., Deane, G. B., Mayol-Bracero, O. L., Grassian, V. H., Bertram, T. H., Bertram, A. K.,  
20 Moffett, B. F. and Franc, G. D.: Sea spray aerosol as a unique source of ice nucleating  
21 particles, *Proc. Natl. Acad. Sci.*, 201514034, doi:10.1073/pnas.1514034112, 2015.
- 22 Dery, S. J. and Yau, M. K.: A climatology of adverse winter-type weather events, *J. Geophys.*  
23 *Res.*, 104672(16), 657–16, doi:10.1029/1999JD900158, 1999.
- 24 Fleming, Z. L., Monks, P. S. and Manning, A. J.: Review: Untangling the influence of air-  
25 mass history in interpreting observed atmospheric composition, *Atmos. Res.*, 104–105, 1–39,  
26 doi:10.1016/j.atmosres.2011.09.009, 2012.
- 27 Gabey, A. M., Gallagher, M. W., Whitehead, J., Dorsey, J. R., Kaye, P. H., and Stanley, W.  
28 R.: Measurements and comparison of primary biological aerosol above and below a tropical  
29 forest canopy using a dual channel fluorescence spectrometer, *Atmos. Chem. Phys.*, 10, 4453–  
30 4466, doi:10.5194/acp-10-4453-2010, 2010.
- 31 Gallet, J. C., Domine, F., Savarino, J., Dumont, M. and Brun, E.: The growth of sublimation



- 1 crystals and surface hoar on the Antarctic plateau, *Cryosphere*, 8(4), 1205–1215,  
2 doi:10.5194/tc-8-1205-2014, 2014.
- 3 Geerts, B., Pokharel, B. and Kristovich, D. a. R.: Blowing Snow as a Natural Glaciogenic  
4 Cloud Seeding Mechanism, *Mon. Weather Rev.*, 143(12), 5017–5033, doi:10.1175/MWR-D-  
5 15-0241.1, 2015.
- 6 Gibson, J. A. E., Garrick, R. C., Burton, H. R. and McTaggart, A. R.: Dimethylsulfide and the  
7 alga *Phaeocystis pouchetii* in antarctic coastal waters, *Mar. Biol.*, 104(2), 339–346,  
8 doi:10.1007/BF01313276, 1990.
- 9 Giordano, M. R., Kalnajs, L. E., Avery, A., Goetz, J. D., Davis, S. M., and DeCarlo, P. F.: A  
10 missing source of aerosols in Antarctica – beyond long-range transport, phytoplankton, and  
11 photochemistry, *Atmos. Chem. Phys.*, 17, 1-20, doi:10.5194/acp-17-1-2017, 2017.
- 12 Good, N., Coe, H. and McFiggans, G.: Instrumentational operation and analytical  
13 methodology for the reconciliation of aerosol water uptake under sub-and supersaturated  
14 conditions, *Atmos. Meas. Tech.*, 3(5), 1241–1254, doi:10.5194/amt-3-1241-2010, 2010.
- 15 Grosvenor, D. P., Choularton, T. W., Lachlan-Cope, T., Gallagher, M. W., Crosier, J., Bower,  
16 K. N., Ladkin, R. S. and Dorsey, J. R.: In-situ aircraft observations of ice concentrations  
17 within clouds over the Antarctic Peninsula and Larsen Ice Shelf, *Atmos. Chem. Phys.*, 12(23),  
18 11275–11294, doi:10.5194/acp-12-11275-2012, 2012.
- 19 Hallett, J. and Mossop, S. C. C.: Production of secondary ice particles during the riming  
20 process, *Nature*, 249(5452), 26–28, doi:10.1038/249026a0, 1974.
- 21 Huang, Y., Blyth, A. M., Brown, P. R. A., Choularton, T. W. and Cui, Z.: Factors Controlling  
22 Secondary Ice Production in Cumulus Clouds, *Q. J. R. Meteorol. Soc.*, 2017.
- 23 Jackson, R. C., McFarquhar, G. M., Korolev, A. V., Earle, M. E., Liu, P. S. K., Lawson, R. P.,  
24 Brooks, S., Wolde, M., Laskin, A., and Freer, M.: The dependence of ice microphysics on  
25 aerosol concentration in arctic mixed-phase stratus clouds during ISDAC and M-PACE, *J.*  
26 *Geophys. Res.*, 117, D15207, doi:10.1029/2012JD017668, 2012.
- 27 Jones, A., Thomson, D., Hort, M. and Devenish, B.: The UK Met Office's next-generation  
28 atmospheric dispersion model, NAME III, *Air Pollut. Model. its ...*, 580–589, 2007.
- 29 Jones, A. E., Wolff, E. W., Salmon, R. A., Bauguitte, S. J. B., Roscoe, H. K., Anderson, P. S.,  
30 Ames, D., Clemithshaw, K. C., Fleming, Z. L., Bloss, W. J., Heard, D. E., Lee, J. D., Read, K.



- 1 A., Hamer, P., Shallcross, D. E., Jackson, A. V., Walker, S. L., Lewis, A. C., Mills, G. P.,
- 2 Plane, J. M. C., Saiz-Lopez, A., Sturges, W. T. and Worton, D. R.: Chemistry of the Antarctic
- 3 Boundary Layer and the Interface with Snow: an overview of the CHABLIS campaign,
- 4 Atmos. Chem. Phys., 8(14), 3789–3803, doi:10.5194/acp-8-3789-2008, 2008.
- 5 Junge, K. and Swanson, B. D.: High-resolution ice nucleation spectra of sea-ice bacteria:  
6 implications for cloud formation and life in frozen environments, Biogeosciences Discuss., 4,  
7 4261–4282, doi:10.5194/bgd-4-4261-2007, 2007.
- 8 King, J. C., Gadian, A., Kirchgaessner, A., Kuipers Munneke, P., Lachlan-Cope, T. A., Orr,  
9 A., Reijmer, C., van den Broeke, M. R., van Wessem, J. M., and Weeks, M.: Validation of the  
10 summertime surface energy budget of Larsen C Ice Shelf (Antarctica) as represented in three  
11 high-resolution atmospheric models, J. Geophys. Res.-Atmos., 120, 1335–1347,  
12 doi:10.1002/2014JD022604, 2015.
- 13 King, J. C., Lachlan-Cope, T. A., Ladkin, R. S. and Weiss, A.: Airborne measurements in the  
14 stable boundary layer over the Larsen Ice Shelf, Antarctica, Boundary-Layer Meteorol.,  
15 127(3), 413–428, doi:10.1007/s10546-008-9271-4, 2008.
- 16 Korolev, A. V., Emery, E. F., Strapp, J. W., Cober, S. G., Isaac, G. A., Wasey, M. and  
17 Marcotte, D.: Small ice particles in tropospheric clouds: Fact or artifact? Airborne icing  
18 instrumentation evaluation experiment, Bull. Am. Meteorol. Soc., 92(8), 967–973,  
19 doi:10.1175/2010BAMS3141.1, 2011.
- 20 Kumai, M.: Identification of Nuclei and Concentrations of Chemical Species in Snow  
21 Crystals Sampled at the South Pole, J. Atmos. Sci., 33(5), 833–841, doi:10.1175/1520-  
22 0469(1976)033<0833:IONACO>2.0.CO;2, 1976.
- 23 Lachlan-Cope, T., Listowski, C., and O'Shea, S.: The microphysics of clouds over the  
24 Antarctic Peninsula – Part 1: Observations, Atmos. Chem. Phys., 16, 15605–15617,  
25 doi:10.5194/acp-16-15605-2016, 2016.
- 26 Lance, S., Brock, C. A., Rogers, D. and Gordon, J. A.: Water droplet calibration of the Cloud  
27 Droplet Probe (CDP) and in-flight performance in liquid, ice and mixed-phase clouds during  
28 ARCPAC, Atmos. Meas. Tech., 3(6), 1683–1706, doi:10.5194/amt-3-1683-2010, 2010.
- 29 Lance, S., Shupe, M. D., Feingold, G., Brock, C. A., Cozic, J., Holloway, J. S., Moore, R. H.,  
30 Nenes, A., Schwarz, J. P., Spackman, J. R., Froyd, K. D., Murphy, D. M., Brioude, J.,  
31 Cooper, O. R., Stohl, A. and Burkhardt, J. F.: Cloud condensation nuclei as a modulator of ice



- 1 processes in Arctic mixed-phase clouds, *Atmos. Chem. Phys.*, 11(15), 8003–8015,  
2 doi:10.5194/acp-11-8003-2011, 2011.
- 3 Lathem, T. L., Beyersdorf, A. J., Thornhill, K. L., Winstead, E. L., Cubison, M. J., Hecobian,  
4 A., Jimenez, J. L., Weber, R. J., Anderson, B. E. and Nenes, A.: Analysis of CCN activity of  
5 Arctic aerosol and Canadian biomass burning during summer 2008, *Atmos. Chem. Phys.*,  
6 13(5), 2735–2756, doi:10.5194/acp-13-2735-2013, 2013.
- 7 Lawson, R. P. and Gettelman, A.: Impact of Antarctic mixed-phase clouds on climate, ,  
8 111(51), doi:10.1073/pnas.1418197111, 2014.
- 9 Lawson, R. P., O'Connor, D., Zmarzly, P., Weaver, K., Baker, B., Mo, Q. and Jonsson, H.:  
10 The 2D-S (stereo) probe: Design and preliminary tests of a new airborne, high-speed, high-  
11 resolution particle imaging probe, *J. Atmos. Ocean. Technol.*, 23(11), 1462–1477,  
12 doi:10.1175/JTECH1927.1, 2006.
- 13 Lawson, R. P., Woods, S. and Morrison, H.: The Microphysics of Ice and Precipitation  
14 Development in Tropical Cumulus Clouds, *J. Atmos. Sci.*, 150310071420004,  
15 doi:10.1175/JAS-D-14-0274.1, 2015.
- 16 Legrand, M., Yang, X., Preunkert, S. and Therys, N.: Year-round records of sea salt, gaseous,  
17 and particulate inorganic bromine in the atmospheric boundary layer at coastal (Dumont  
18 d'Urville) and central (Concordia) East Antarctic sites, *J. Geophys. Res. Atmos.*, 121(2), 997–  
19 1023, doi:10.1002/2015JD024066, 2016.
- 20 Listowski, C. and Lachlan-Cope, T.: The Microphysics of Clouds over the Antarctic  
21 Peninsula – Part 2: modelling aspects within Polar WRF, *Atmos. Chem. Phys. Discuss.*,  
22 doi:10.5194/acp-2016-1135, in review, 2017.
- 23 Liu, D., Quennehen, B., Darbyshire, E., Allan, J. D., Williams, P. I., Taylor, J. W., J.-B.  
24 Bauguitte, S., Flynn, M. J., Lowe, D., Gallagher, M. W., Bower, K. N., Choularton, T. W. and  
25 Coe, H.: The importance of Asia as a source of black carbon to the European Arctic during  
26 springtime 2013, *Atmos. Chem. Phys.*, 15(20), 11537–11555, doi:10.5194/acp-15-11537-  
27 2015, 2015.
- 28 Lloyd, G., Choularton, T. W., Bower, K. N., Crosier, J., Jones, H., Dorsey, J. R., Gallagher,  
29 M. W., Connolly, P., Kirchgaessner, A. C. R. and Lachlan-Cope, T.: Observations and  
30 comparisons of cloud microphysical properties in spring and summertime Arctic  
stratocumulus clouds during the ACCACIA campaign, *Atmos. Chem. Phys.*, 15(7), 3719–



- 1 3737, doi:10.5194/acp-15-3719-2015, 2015a.
- 2 Lloyd, G., Choularton, T. W., Bower, K. N., Gallagher, M. W., Connolly, P. J., Flynn, M.,  
3 Farrington, R., Crosier, J., Schlenczek, O., Fugal, J. and Henneberger, J.: The origins of ice  
4 crystals measured in mixed phase clouds at High-Alpine site Jungfraujoch, Atmos. Chem.  
5 Phys. Discuss., 15(13), 18181–18224, doi:10.5194/acpd-15-18181-2015, 2015b.
- 6 Lubin, D., Chen, B., Bromwich, D. H., Somerville, R. C. J., Lee, W. H. and Hines, K. M.:  
7 The impact of antarctic cloud radiative properties on a GCM climate simulation, J. Clim.,  
8 11(3), 447–462, doi:10.1175/1520-0442(1998)011<0447:TIOACR>2.0.CO;2, 1998.
- 9 Mahesh, A.: Observations of blowing snow at the South Pole, J. Geophys. Res., 108(D22), 1–  
10 9, doi:10.1029/2002JD003327, 2003.
- 11 Mauritsen, T., Sedlar, J., Tjernström, M., Leck, C., Martin, M., Shupe, M., Sjogren, S.,  
12 Sierau, B., Persson, P. O. G., Brooks, I. M. and Swietlicki, E.: An Arctic CCN-limited cloud-  
13 aerosol regime, Atmos. Chem. Phys., 11(1), 165–173, doi:10.5194/acp-11-165-2011, 2011.
- 14 McFarquhar, G. M. and Cober, S. G.: Single-scattering properties of mixed-phase Arctic  
15 clouds at solar wavelengths: Impacts on radiative transfer, J. Clim., 17(19), 3799–3813,  
16 doi:10.1175/1520-0442(2004)017<3799:SPOMAC>2.0.CO;2, 2004.
- 17 McFarquhar, G. M., Zhang, G., Poellot, M. R., Kok, G. L., McCoy, R., Tooman, T., Fridlind,  
18 A. and Heymsfield, A. J.: Ice properties of single-layer stratocumulus during the Mixed-Phase  
19 Arctic Cloud Experiment: 1. Observations, J. Geophys. Res. Atmos., 112(24), 1–19,  
20 doi:10.1029/2007JD008633, 2007.
- 21 Möhler, O., Field, P. R., Connolly, P., Benz, S., Saathoff, H., Schnaiter, M., Wagner, R.,  
22 Cotton, R., Krämer, M., Mangold, A., and Heymsfield, A. J.: Efficiency of the deposition  
23 mode ice nucleation on mineral dust particles, Atmos. Chem. Phys., 6, 3007–3021,  
24 doi:10.5194/acp-6-3007-2006, 2006.
- 25 Möhler, O., DeMott, P. J., Vali, G. and Levin, Z.: Microbiology and atmospheric processes:  
26 the role of biological particles in cloud physics, Biogeosciences Discuss., 4(4), 2559–2591,  
27 doi:10.5194/bgd-4-2559-2007, 2007.
- 28 Morrison, H., Thompson, G. and Tatarkii, V.: Impact of Cloud Microphysics on the  
29 Development of Trailing Stratiform Precipitation in a Simulated Squall Line: Comparison of  
30 One- and Two-Moment Schemes, Mon. Weather Rev., 137(3), 991–1007,



- 1      doi:10.1175/2008MWR2556.1, 2009.
- 2      Mossop, S. C.: Secondary ice particle production during rime growth: The effect of drop size  
3      distribution and rimer velocity, *Q. J. R. Meteorol. Soc.*, 111(470), 1113–1124,  
4      doi:10.1002/qj.49711147012, 1985.
- 5      Mossop, S. C. and Hallett, J.: Ice crystal concentration in cumulus clouds: influence of the  
6      drop spectrum., *Science* (80-.), 186(1963), 632–634, doi:10.1126/science.186.4164.632,  
7      1974.
- 8      Mossop, S. C. C.: Production of secondary ice particles during the growth of graupel by  
9      riming, *Nature*, (102), 45–57, doi:10.1038/249026a0, 1976.
- 10     Murray, B. J., O’Sullivan, D., Atkinson, J. D. and Webb, M. E.: Ice nucleation by particles  
11     immersed in supercooled cloud droplets., *Chem. Soc. Rev.*, 41(19), 6519–54,  
12     doi:10.1039/c2cs35200a, 2012.
- 13     Niemand, M., Möhler, O., Vogel, B., Vogel, H., Hoose, C., Connolly, P., Klein, H.,  
14     Bingemer, H., DeMott, P., Skrotzki, J. and Leisner, T.: A Particle-Surface-Area-Based  
15     Parameterization of Immersion Freezing on Desert Dust Particles, *J. Atmos. Sci.*, 69(10),  
16     3077–3092, doi:10.1175/JAS-D-11-0249.1, 2012.
- 17     Palm, S. P., Yang, Y., Spinhirne, J. D. and Marshak, A.: Satellite remote sensing of blowing  
18     snow properties over Antarctica, *J. Geophys. Res. Atmos.*, 116(16), 1–16,  
19     doi:10.1029/2011JD015828, 2011.
- 20     Petters, M. D. and Kreidenweis, S. M.: A single parameter representation of hygroscopic  
21     growth and cloud condensation nucleus activity, *Atmos. Chem. Phys.*, (7), 1961–1971,  
22     doi:10.5194/acp-13-1081-2013, 2007.
- 23     Pringle, K. J., Tost, H., Pozzer, A., Pöschl, U., and Lelieveld, J.: Global distribution of the  
24     effective aerosol hygroscopicity parameter for CCN activation, *Atmos. Chem. Phys.*, 10,  
25     5241–5255, doi:10.5194/acp-10-5241-2010, 2010.
- 26     Rosenberg, P. D., Dean, a. R., Williams, P. I., Dorsey, J. R., Minikin, a., Pickering, M. a.  
27     and Petzold, a.: Particle sizing calibration with refractive index correction for light scattering  
28     optical particle counters and impacts upon PCASP and CDP data collected during the Fennec  
29     campaign, *Atmos. Meas. Tech.*, 5(5), 1147–1163, doi:10.5194/amt-5-1147-2012, 2012.
- 30     Taylor, J. W., Choularton, T. W., Blyth, A. M., Liu, Z., Bower, K. N., Crosier, J., Gallagher,



- 1 M. W., Williams, P. I., Dorsey, J. R., Flynn, M. J., Bennett, L. J., Huang, Y., French, J.,
- 2 Korolev, A., and Brown, P. R. A.: Observations of cloud microphysics and ice formation
- 3 during COPE, *Atmos. Chem. Phys.*, 16, 799–826, doi:10.5194/acp-16-799-2016, 2016.
- 4 Thorpe, A. D. and Mason, B. J.: The evaporation of ice spheres and ice crystals, *Br. J. Appl.*
- 5 *Phys.*, 17(4), 541, doi:10.1088/0508-3443/17/4/316, 1966.
- 6 Topping, D. O., McFiggans, G. B. and Coe, H.: A curved multi-component aerosol
- 7 hygroscopicity model framework: Part 1 – Inorganic compounds, , 1205–1222, 2005.
- 8 Vali, G., Leon, D. and Snider, J. R.: Ground-layer snow clouds, *Q. J. R. Meteorol. Soc.*,
- 9 138(667), 1507–1525, doi:10.1002/qj.1882, 2012.
- 10 Verlinde, J., Harrington, J. Y., McFarquhar, G. M., Yannuzzi, V. T., Avramov, A.,
- 11 Greenberg, S., Johnson, N., Zhang, G., Poellot, M. R., Mather, J. H., Turner, D. D., Eloranta,
- 12 E. W., Zak, B. D., Prenni, A. J., Daniel, J. S., Kok, G. L., Tobin, D. C., Holz, R., Sassen, K.,
- 13 Spangenberg, D., Minnis, P., Tooman, T. P., Ivey, M. D., Richardson, S. J., Bahrmann, C. P.,
- 14 Shupe, M., DeMott, P. J., Heymsfield, A. J. and Schofield, R.: The mixed-phase arctic cloud
- 15 experiment, *Bull. Am. Meteorol. Soc.*, 88(2), 205–221, doi:10.1175/BAMS-88-2-205, 2007.
- 16 Virkkula, A. and Teinil, K.: Chemical composition of boundary layer aerosol over the
- 17 Atlantic Ocean and at an Antarctic site, *Atmos. Chem. Phys.*, (January 2000), 3407–3421,
- 18 2006.
- 19 Weller, R., Wöltjen, J., Piel, C., Resenberg, R., Wagenbach, D., König-Langlo, G. and
- 20 Kriewa, M.: Seasonal variability of crustal and marine trace elements in the aerosol at
- 21 Neumayer station, Antarctica, *Tellus, Ser. B Chem. Phys. Meteorol.*, 60 B(5), 742–752,
- 22 doi:10.1111/j.1600-0889.2008.00372.x, 2008.
- 23 Weller, R., Minikin, A., Wagenbach, D. and Dreiling, V.: Characterization of the inter-
- 24 annual, seasonal, and diurnal variations of condensation particle concentrations at Neumayer,
- 25 Antarctica, *Atmos. Chem. Phys.*, 11(24), 13243–13257, doi:10.5194/acp-11-13243-2011,
- 26 2011.
- 27 Whitehead, J. D., Darbyshire, E., Brito, J., Barbosa, H. M. J., Crawford, I., Stern, R.,
- 28 Gallagher, M. W., Kaye, P. H., Allan, J. D., Coe, H., Artaxo, P. and McFiggans, G.: Biogenic
- 29 cloud nuclei in the Amazon, *Atmos. Chem. Phys. Discuss.*, (January), 1–23, doi:10.5194/acp-
- 30 2015-1020, 2016.



- 1 Wilson, T. W., Ladino, L. A., Alpert, P. A., Breckels, M. N., Brooks, I. M., Browse, J.,
  - 2 Burrows, S. M., Carslaw, K. S., Huffman, J. A., Judd, C., Kilthau, W. P., Mason, R. H.,
  - 3 McFiggans, G., Miller, L. A., Najera, J., Polishchuk, E., Rae, S., Schiller, C. L., Si, M.,
  - 4 Vergara Temprado, J., Whale, T. F., Wong, J. P. S., Wurl, O., Yakobi-Hancock, J. D., Abbatt,
  - 5 J. P. D., Aller, J. Y., Bertram, A. K., Knopf, D. A. and Murray, B. J.: A marine biogenic
  - 6 source of atmospheric ice nucleating particles, *Nature*, doi:10.1038/nature14986, 2015.
  - 7 Xu, L., Russell, L. M., Somerville, R. C. J., and Quinn, P. K.: Frost flower aerosol effects on
  - 8 Arctic wintertime longwave cloud radiative forcing, *J. Geophys. Res.-Atmos.*, 118, 13282–
  - 9 13291, doi:10.1002/2013JD020554, 2013.
  - 10 Yang, X., Pyle, J. A. and Cox, R. A.: Sea salt aerosol production and bromine release: Role of
  - 11 snow on sea ice, *Geophys. Res. Lett.*, 35(16), 1–5, doi:10.1029/2008GL034536, 2008.
  - 12 Yano, J.-I. and Phillips, V. T. J.: Ice–Ice Collisions: An Ice Multiplication Process in
  - 13 Atmospheric Clouds, *J. Atmos. Sci.*, 68(2), 322–333, doi:10.1175/2010JAS3607.1, 2011.
- 14